

NPS ARCHIVE  
1967  
MOULSON, J.

NUCLEATE POOL BOILING OF NITROGEN  
FROM ARTIFICIAL CAVITIES

JOHN ALFRED MOULSON








NUCLEATE POOL BOILING OF NITROGEN  
FROM ARTIFICIAL CAVITIES

by

John Alfred Moulson  
Lieutenant, United States Navy  
B.S., Massachusetts Institute of Technology, 1962



Submitted in partial fulfillment of the  
requirements for the degree of

MASTER OF SCIENCE IN MECHANICAL ENGINEERING

from the

NAVAL POSTGRADUATE SCHOOL  
September 1967

167  
OULSON, J.

14855  
c1

Abstract

NUCLEATE POOL BOILING OF NITROGEN FROM ARTIFICIAL CAVITIES

Pool boiling heat transfer of nitrogen from artificial cavities was investigated. Boiling was from circular, one inch diameter horizontal mirror finished copper plates.

The single artificial cavity surfaces investigated were: a drilled 0.0043 inch diameter hole, a drilled 0.015 inch diameter hole, an 0.022 inch diameter spark cut cone, and an 0.006 inch diameter spark cut cylindrical hole. The multiple cavity surfaces investigated were: seven 0.015 inch diameter drilled holes, thirteen 0.015 inch diameter drilled holes, and ninety-seven 0.003 to 0.0045 inch diameter spark cut holes. The depth to diameter ratio was about 2.5 for all drilled cavities.

The data from a mirror finished surface was compared to that of previous investigations. Exponents for Yamagata's Equation for boiling in the isolated bubble region were determined. The artificial cavities were found to affect the natural convection heat transfer. The size of the cavity appeared to have little effect after incipience of boiling, and larger cavities than previously expected were found to remain active.

TABLE OF CONTENTS

SECTION	PAGE NO.
1. INTRODUCTION	11
1.1 Background	11
1.2 Previous Research	12
2. APPARATUS	15
2.1 System	15
2.2 Boiler Diaphragms	16
2.3 Boiler Plates	16
2.4 Temperature Measurement System	17
3. EXPERIMENTAL	19
3.1 Test Surface Preparation	19
3.1.1 Mirror Finish	19
3.1.2 Cylindrical Cavities	20
3.1.3 Conical Cavity	23
3.2 Test Surface Installation	23
3.3 Testing Procedures	24
3.3.1 Reproducibility and Q/A vs $\Delta T$ Curves	24
3.3.2 Boiling only from Artificial Cavities	24
3.4 Microscopic Examination of Surfaces	25
4. RESULTS	27
4.1 Natural Convection	27
4.2 Hysteresis	28
4.3 Reproducibility	30
4.4 Single Cylindrical Cavities	30

4.5	Conical Cavity	32
4.6	Multiple Spark Cut Holes	32
4.7	Multiple Drilled Holes	33
5.	CONCLUSIONS AND RECOMMENDATIONS	36
	BIBLIOGRAPHY	39
	APPENDICES	
	A. Thermocouple Calibration	41
	B. Thermocouple Calibration Program	46
	C. Sample Calculation with Error Analysis	53



## LIST OF TABLES

TABLE		PAGE
3-1	Summary of Procedures	24
4-1	Comparison of Exponents for the Yamagata Equation	35
A-1	Thermocouple Calibration Summary	43
A-2	Comparison of Calibration Data	44
B-1	Thermocouple Table	52
C-1	Thermocouple Data	53
C-2	Error Summary	55



## LIST OF FIGURES

FIGURE		PAGE
1.	Characteristic Boiling Curve	59
2.	Schematic of System	60
3.	Test Surface Assembly	61
4.	Thermocouple Well Locations	62
5.	Thermocouple Control System	63
6.	Layout of Thirteen Drilled Cavities	64
7.	Layout of Ninety-Seven Spark Cut Cavities	65
8.	Photographs of Spark Cut Hole Mouths	66
9.	Photographs of Cross-Section of Spark Cut Hole	67
10.	Natural Convection Data Showing Jump Effect Obtained with Single Drilled Cavities	68
11.	Time-Temperature-Heat Flux Plot	69
12.	Effect on the Boiling Curves of Different Time Intervals between Power Level Changes	70
13.	Curve Showing Reproducibility of Boiling Data Using Mirror Finish Surfaces	71
14.	Mirror Finish Boiling Curve Showing other Experimenters' Mirror Finish Data	72
15.	Effect on the Boiling Curve of Different Sizes of Cylindrical Cavities	73
16.	Effect of Cavity Geometry on the Boiling Curve	74
17.	Effect of Spark Cut Cavities on the Boiling Curve	75
18.	Effect of Number of Drilled Cavities on the Boiling Curve	76
19.	Comparison of Boiling Only from Artificial Cavities to Natural Convection Curves	77

20.	Boiling Only from Artificial Cavities Data Showing Curves Obtained Using Yamagata's Equation	78
21.	Sample Temperature - EMF Curve	79
22.	Thermal Conductivity of Copper	80
23.	Temperature Distribution in the Boiler Cylinder	81

## LIST OF SYMBOLS

SYMBOL	DEFINITION
A	Area, $\text{cm}^2$
C	Constant
P	Pressure, mm Hg
Q	Heat, BTU/hr or watts
T	Temperature, degrees Kelvin
a	Nucleate Boiling Exponent
b	Nucleate Boiling Exponent
k	Thermal Conductivity, $\text{watts/cm-}^\circ\text{K}$
n	Number of Active Sites
x	Natural Convection Exponent
n/A	Active Site Density, $\text{cm}^{-2}$
Q/A	Heat Flux, $\text{watts/cm}^2$
dT/dx	Temperature Gradient, $^\circ\text{K/cm}$

## SUBSCRIPTS

atm	Atmosphere
head	Head
sat	Saturation
tot	Total
w	Wall

## Acknowledgements

The author wishes to express his gratitude for the assistance and encouragement given him by Professor P. J. Marto. He also wishes to thank Messrs. H. Perry and F. Abbe for their many hours in the Machine Shop and Messrs. K. Smith and J. Beck for their help with the cryogenic and vacuum work. Special thanks go to Mr. Kenneth Motherseil for his fine work and assistance in all phases of this project.

SECTION I  
INTRODUCTION

1.1 Background - Liquid nitrogen and other cryogenic fluids have been gaining a wide role in industry and research programs. Their uses vary from space vessel fuels and gas separation techniques to electromagnetic coolers.

The characteristics of cryogenic fluids undergoing boiling vary greatly from those of ordinary fluids. This is due, in part, to the fact that the properties of both the cryogenic fluids and the heating surfaces involved with them differ from those conventionally encountered. The heat fluxes and temperature differences associated with boiling are smaller and heats of vaporization are lower. Structural materials have lower specific heats, giving rise to rapid temperature increases and film boiling.

Boiling heat transfer data is generally presented graphically with  $\log (Q/A)$  as ordinate and  $\log (\Delta T)$  as abscissa where  $\Delta T$  is the temperature difference between the solid surface in contact with the fluid ( $T_w$ ) and the fluid saturation temperature ( $T_{sat}$ ). The data thus plotted yields the familiar characteristic boiling curve (Figure 1) which has the same shape for all fluids. There are four boiling regimes on this curve, depending on heat flux and temperature difference of operation.

Natural convection occurs at low superheats (temperature differences) and is generally associated with low heat fluxes. The driving force for fluid motion is due to the buoyant force created by a fluid density change. The fluid expands as it is heated by the plate and consequently rises. For large horizontal surfaces with natural con-

vection the obtainable heat flux is proportional to the temperature difference between the wall and the fluid bulk raised to the 1.25 to 1.33 power (1).

Nucleate boiling is characterized by a sharp rise in the heat transfer coefficient due to fluid agitation by rapidly growing and departing bubbles. This regime is of the most practical importance since it provides for the transfer of large amounts of heat with small temperature differences. Almost all industrial equipment utilizing boiling heat transfer is designed for operation in this regime.

Transition boiling is characterized by a lowering of the heat transfer coefficient with increasing temperature difference. This is an unstable region. Berenson (2) in his investigation found that the liquid occasionally touches the surface but generally it is supported by an unstable vapor blanket.

The stable film boiling regime is characterized by an orderly discharge of large bubbles from the film at regular intervals. The heat flux again increases with an increase of surface temperature, but at a slower rate than in nucleate boiling.

1.2 Previous Research - Since the discovery of the characteristic boiling curve by Nukiyama in 1934 there has been a great proliferation of boiling heat transfer research.

In the nucleate boiling region many factors have been found to affect the shape of the boiling curve. Among these are surface conditions, contaminants, boiling history and boiler surface material.

Mead, Romie and Guibert (3) were among the first to suggest that surface roughness or trapped gases on the surface would lower the



superheat and change the boiling curve. Corty and Foust (4) investigated boiling organic liquids using a transparent container. They noted hysteresis effects and shifting of the boiling curve to give lower superheats. Griffith and Wallis (5) tried to correlate bubble size, shape and frequency to the wall superheat required for bubble growth by their studies of surfaces punched with needles. Bonilla, Grady and Avery (6) investigated the effects of scratches and tried to correlate scratch spacing to bubble size. Others investigated wetting agents, non-wetting surfaces, gravity effects, etc.

Research in boiling cryogenic fluids has been more limited due to the added problems associated with extreme cold and the lack of interest until only recently. Class and others (7) studied boiling hydrogen heat transfer from surfaces coated with grease and tilted at various angles. Oxygen and nitrogen investigations were conducted by Lyon (8). Kosky (9) boiled nitrogen over a wide pressure range from platinum plates. Almgren and Smith (10) investigated roughened surfaces, boiling inception and hysteresis (the effect of past heating history on the boiling curve) while boiling nitrogen from a horizontal plate in their investigation of pressure effects. Other experimenters using liquid nitrogen studied peak nucleate boiling flux and boiling from wires (11). The forerunners of this current project, Maynard (12) and George (13) investigated the effects of surface contaminants (grease), different surface materials, etched surfaces and single cylindrical cavities.

A correlation of nucleate boiling heat transfer based on dimensional analysis and a surface variable constant was developed by Rohsenow (14). Forster and Zuber (15) also produced a correlation based on non-dimensional parameters. However, neither of these nor the many others

that have been developed fully account for all the variables such as dissolved gases, impurities, contaminants, and surface conditions. The available data are scattered due to the large number of variables involved making correlation very difficult.

The primary objective of this project was to investigate the effects of cavity size and density on the characteristic boiling curve of liquid nitrogen.

## SECTION 2

### APPARATUS

2.1 System - The system used for conducting cryogenic boiling tests was conceived by M. D. Maynard (12). It was designed with versatility to cover a wide range of tests, including boiling at reduced pressures and with the ability to eventually conduct boiling tests using liquid helium.

Essentially the system consisted of an outer dewar, which contained liquid nitrogen in this case. This provided an adiabatic inner chamber.

The inner dewar contained the liquid to be boiled; a tube and can arrangement which contained the heater, test surface, and a temperature sensing device was also immersed in the inner dewar. A primary vacuum system was used to evacuate the tube and can to reduce heat losses and a secondary vacuum system for pool environmental control. There were various temperature and pressure sensing devices to monitor the systems and to obtain the desired data.

Figure 2 is a schematic of the system. A further description of the system components designed by Maynard and George appears in reference (13). The apparatus which was modified by this author is listed below.

Three major modifications were made to improve the system; the first two were made to improve the surfaces being tested and to eliminate the need for electroplating them by providing a single piece test surface and strengthening the diaphragm. The third modification was made to provide more reliable thermocouple data by eliminating solder joints.

2.2 Boiler Diaphragms - The boiler diaphragm shown in Figure 3 was used to support the boiler in the boiler enclosure. It was a flat disc made from Nickel 200 and was designed to provide for easy replacement of boiler plates. George (13) initially designed these plates. It was noted, however, that they tended to bend near the center when installed. The inner portion, formally 0.023 inches thick was redesigned to 0.048 inches. This section was originally designed to be as thin as possible to prevent heat loss due to thermal conduction horizontally from the boiler plate.

2.3 Boiler Plates - The boiler plates were manufactured from electrolytic tough pitch (ETP) copper. They consisted of a cylinder  $2 \frac{3}{8}$  inches diameter and one inch long which was machined for 0.835 inches of its length to a diameter of 0.993 inches. In each case the top of the plate, 0.165 inches long and  $2 \frac{3}{8}$  inches in diameter, was soldered on its underside to the topside of the boiler diaphragm. The top was then machined to a final thickness of 0.015 inches. Figure 3 shows this assembly. The thickness was kept to a maximum of 0.015 inches to prevent large horizontal heat losses.

The wide top was provided to eliminate the transition ring (solder ring) which occurred in both Maynard's and George's boilers and to eliminate the need for electroplating them. Their test surfaces were designed with the nickel diaphragm serving as part of the surface. The boiler cylinder was soldered to the diaphragm at the top, thus, the test surface consisted of three materials - copper in the center, a solder ring, and nickel on the edge. Rogue nucleation sites existed in the solder ring due to its porosity. George electroplated his surfaces with copper to fill in the porous sections in order to eliminate these sites.

The length of the small diameter section was selected so as to give a reasonable temperature gradient between the boiler surface and the bottom of the cylinder to allow accurate temperature gradient and, thus, heat flux measurements.

Four thermocouple holes, spaced  $90^{\circ}$  apart, were drilled in the lower part of the cylinder. They were 0.035 inches diameter and 0.495 inches deep and spaced as shown in Figure 4.

2.4 Temperature Measurement System - Temperature measurement was considered to be critical with highest degree of accuracy being required. Thus, ISA type T copper-constantan thermocouples sheathed in stainless steel (Sheath diameter = 0.035 inches) with special limits of error were selected. The thermocouples were six feet long and each had a grounded junction.

Metal sheathing was at first considered necessary in order to limit outgassing in the thermal insulation vacuum system. However, normal, small diameter, high grade glass insulated thermocouples would probably be more satisfactory in that zero resistance (shorting) problems would be reduced.

The thermocouples were rewired as shown in Figure 5. This was done to eliminate stray emfs from soldered joints in the zone box. The new system eliminated the zone box (an insulated container used to keep all bimetallic connections at the same temperature) and rotary switch and provided each thermocouple with its own reference junction. Baker, Ryder and Baker (16) suggest using knife-edge switches in lieu of a rotary switch and to eliminate all soldered connections. All copper wire was attached to magnanin binding posts which have low thermal emfs, and all constantan wires were wound together. After calibration

(Appendix A), four thermocouples were passed through the Conax gland and into the boiler enclosure where they were coated with silicone vacuum grease and inserted into the boiler plates to full depth (0.495 inches). The fifth thermocouple was inserted in the liquid nitrogen about three inches above the test surface to provide a check on the liquid bulk temperature.

The knife switches were connected together and to a Leeds and Northrup K-3 potentiometer by heavy copper thermocouple lead wire.

The five reference junctions were enclosed in plastic and inserted in a sealed eight inch long oil-filled copper tube which was immersed in a crushed ice-water bath. An ice-water reference junction was used because it was more stable than any other convenient reference point.

The above temperature monitoring system was very satisfactory and its inherent error was estimated to be less than  $0.25^{\circ}$  K (4.0 microvolts) over long periods of time (twelve or more hours) and accurate to within  $0.05^{\circ}$  K over shorter periods.

Data was hand-recorded from the K-3 potentiometer using the null method.

## SECTION 3

### EXPERIMENTAL

3.1 Test Surface Preparation - After assembly of test surfaces, as outlined in the previous section, each surface was cleaned with acetone. The surfaces were prepared for testing as outlined below.

3.1.1 Mirror Finish - The boiler test surface was first dry sanded using emery paper and then wet polished on several metallurgical wheels in order to obtain a mirror finish surface.

A high speed belt sander (320 grit carborundum) was used to remove all traces of machining. The sample was then rotated  $90^{\circ}$  and hand sanded on dry 0 emery paper, rotated  $90^{\circ}$  and sanded on dry 2/0 emery paper. Final dry sanding was on 3/0 emery paper after again rotating the surface  $90^{\circ}$ . The sample was then washed with detergent and warm water to remove all grit.

Wet polishing was accomplished on four inch Buehler metallurgical polishing wheels. On every wheel the specimen was placed face down for several minutes. It was then lifted, rinsed, rotated  $180^{\circ}$  and replaced on that same wheel for several more minutes. Between wheels the specimen was washed with detergent and warm water to remove the previous abrasive. The first wheel was canvas covered and used a 600 grit carborundum-water suspension as abrasive. The second wheel was covered with felt and used an alumina-water suspension as abrasive. The third wheel was covered with kitten ear, a felt-like material, and used one micron gamma-alumina in water as an abrasive. The last two wheels were covered with velvet. They were impregnated with three micron and one micron diamond dust, respectively. For these wheels, methanol was used to wet the surfaces.

After completion of the polishing, the sample was washed with methanol and wrapped in lens paper to prevent contamination.

All surfaces with artificial cavities were mirror finished before the cavities were made and were repolished on the last two wheels after work was completed. This was done to insure that defects incurred in the manufacturing process were not responsible for the change in the boiling curve.

3.1.2 Cylindrical Cavities - Several plates were made with artificial cylindrical cavities to investigate their effect on the boiling characteristics. Both the density and hole size were varied in several different boiler surfaces.

Cavities were drilled using Sphinx spirec pivot drills in two sizes, 0.0043 inch diameter and 0.015 inch diameter. The depth of the cavity was controlled by using a feeler gauge on the lathe.

A cavity depth/diameter ratio of approximately 2.5 was desired. Thus, the 0.0043 hole was drilled to a depth of between 0.012 and 0.015 inches. The 0.015 inch holes were between 0.035 and 0.040 inches deep.

Two plates were prepared with single cavities of the above sizes. Later, an additional plate was made with seven 0.015 inch holes, one in the center of the plate and the other six equally spaced on a  $\frac{1}{2}$  inch diameter circle concentric to the plate. The holes were thus spaced  $\frac{1}{4}$  inch apart. This plate was then tested as outlined below and returned for the placement of six additional holes. The thirteen holes were equally spaced 0.145 inches apart. Figure 6 is a sketch showing the final hole placement.

One of the original seven holes was damaged in manufacture. A drill was broken in the bottom of the hole about 0.025 inches from the mouth.



A second hole was drilled at an angle through the top of the original hole. This slightly enlarged the mouth of the cavity and the internal imperfections caused it to boil differently than the others (it produced smaller diameter bubbles at higher frequency).

Cylindrical cavities were also spark cut into the test surfaces. The Servomet spark cutter manufactured by Metals Research Ltd. was used in this process. A single cavity with estimated mouth diameter 0.003-0.004 inches and estimated depth of 0.010 inches was placed in the center of a boiler plate by using an 0.0016 inch Sphinx flat pivot drill (manufactured by Levin and Son, Inc.) as an electrode. Drills were chosen as electrodes because of their relatively high stiffness and ease of handling as compared to similar sized wire. The drill extended from a shank with a diameter of 0.040 inches. The shank was placed in a specially made tool where it was held with a set screw.

The electrode was allowed to penetrate to a depth of 0.012 inches. The depth of electrode penetration was controlled by using the machine's depth gage micrometer attachment. The spark gap control was set on number seven, the finest spark the machine can produce. The dielectric in the spark cutter was freshly filtered kerosene.

Ninety-seven holes were simultaneously spark cut into a plate using the above-mentioned electrodes and spark cutter. The holes were uniformly distributed within a 0.990 inch diameter circle. This provided a hole center-to-center spacing of 0.095 inches. Figure 7 is a schematic of the hole layout.

A special tool was manufactured to hold the ninety-seven drills in place and at equal distances from the surface. A 2½ inch diameter, 0.600 inch thick plate was cut from naval brass bar stock. The piece

was drilled straight through at the hole locations using an 0.030 inch drill. The piece was then drilled and tapped for machine screws. It was sectioned through its thickness into two parts, one 0.350 inches thick, the other 0.250 inches thick. The holes in the thicker section were redrilled to 0.040 inches diameter. The two pieces were then fastened together using machine screws at the previously placed taps. This procedure insured that the holes in the two plates were coincidental. The Sphinx drills were forced into the 0.040 inch holes and were bottomed off center in the 0.030 inch holes. The drill tips were not allowed to touch either plate as they are very easily broken off. After completion of insertion the drill shanks were soldered into place in the 0.350 inch thick plate. After soldering it was found that the drills extended to somewhat different lengths from the plate.

In order to insure that the test surface and electrode plate were parallel, an electrical contact test was used. Two brass screws 180° apart were set into the electrode surface near its outer edge. They were set so that they stuck out equal distances from the electrode surface. Electrical lead wires were then attached to the screws and to an ohmmeter. The plate was fastened to an end of a 5 x ¼ x ½ inch arm which was then clamped into place on the spark cutter servo drive. The test plate was placed directly below it on the support stand. The servo was then driven down until one of the set screws touched the test surface (the spark cutting machine shuts off when pressure is applied to the electrode). The electrode plate was then moved until a short was indicated on the ohmmeter (both screws touching the test surface). It is estimated that the plate and test surface were parallel to within  $\pm 0.001$  inches.

3.1.3 Conical Cavity - A conical cavity was placed in a test surface by using the spark cutter described above. In this case the electrode was made from a 1/16 inch steel rod turned down to 0.015 inches diameter and tapered at the end. The tapered section was 0.060 inches long to give the desired hole depth of 0.035-0.040 inches. The hole thus made was not truly conical, as the bottom had a fairly large radius of curvature.

3.2 Test Surface Installation - Immediately before installation in the test rig all plates with cavities were put in an ultrasonic cleaner for several minutes, after which they were washed with water, rinsed with ethanol and dried.

A test surface was placed on the boiler can where heater leads, thermocouple junctions and teflon seal were installed. Silicone vacuum grease was put into the thermocouple holes to insure good thermal contact. The thermocouples and heater leads were then checked with an ohmmeter to insure that there were no short circuits. The test surface was then secured to the can by eight 3/16 inch stainless steel studs which were torqued to a maximum of ten inch-pounds (Figure 4). It was found that higher torques warped the plate at the thin nickel ring-copper cylinder junction (Figure 3) causing a small ring to appear on the test surface. This "stress ring" was found to be a source of rogue nucleation sites.

The vacuum system was then started. If, after several minutes the pressure had not dropped to  $10^{-4}$  mm Hg, there was a leak. Tests were not conducted on any surfaces where the pressure exceeded  $10^{-3}$  mm Hg. In such cases the test rig was disassembled and the teflon seal replaced. In every case of excessive leakage, upon opening of the can, one found

that the teflon seal had ripped. After obtaining a satisfactory vacuum, the two dewars were mounted and filled with nitrogen. The outer dewar was filled to within one inch of its top; the inner one was filled to a depth of about 20 cm.

### 3.3 Testing Procedures

3.3.1 Reproducibility and Q/A vs. (Tw-Tsat) Curves - Initial testing was performed with mirror finish plates to determine the best procedures for obtaining reproducible data. Among the factors varied in these runs were liquid depth, amount of preboiling (degassing), time interval between power level changes, and power level increments.

Observations from these tests led to the development of the following test procedure for obtaining heat flux versus temperature difference data.

TABLE 3 - 1

Initial Liquid Depth	20 cm
Preboiling Time	15 - 20 minutes (in order to obtain 16 cm depth at start of run)
Preboiling Power Level	62.5 watts
Cooling Down Time	15 minutes
Power Levels for Run	0.6, 1.25, 2.5, 4.0, 5.6, 7.5, 10.0, 12.5, 15.6, 18.0, 22.5, 40.0, 62.5, 90.0 watts
Time Interval between Power Level Changes	7 minutes (5 minutes plus 2 minutes to take data)

3.3.2 Boiling Only from Artificial Cavities - After some experience was gained in running the tests and observing numbers of active sites, it was found that there was, with the 0.015 inch cylindrical holes, a wide range of power levels where only the artificial cavities were active.

It was then decided that a  $Q/A$  vs  $(T_w - T_{sat})$  curve could be established for these plates with fixed numbers of nucleating sites.

Thus, immediately after taking the last data for the previously described test, the plate was allowed to come to equilibrium with power input of 10 watts. After five minutes the power was lowered slowly to the point where the artificial cavity sites appeared to be on the brink of snuffing out. The power level was then raised to the next highest power level listed in the previous subsection. The procedure outlined there was then followed until natural sites became active, at which point the test was discontinued.

3.4 Microscopic Examination of Surfaces - After completion of the runs, the plates with spark cut cavities were brought to the metallurgical laboratory for examination. The holes were examined under the microscope to determine their shape and size. The single cylindrical cavity had a mouth diameter of 0.007-0.008 inches; the 97 holes were all approximately 3.0-4.5 thousandths across their largest dimension. However, their shapes varied considerably. Crescents, ovals, circles and some completely irregular shapes were observed. Several of these holes appeared to be nothing more than shallow surface scratches as the bottoms were not out of the depth of field when examining the mouth by looking straight down onto the test surface. The shallow holes were probably caused by inconsistent drill lengths extending from the plate. The irregular holes were probably due to solder dripping through the plate and hardening on the drill tips. Figures 8 and 9 are photographs of a typical hole mouth and a cross section.

The conical cavity had a circular mouth 0.022 inches in diameter.

Unfortunately this cavity was accidentally destroyed during sectioning, and no measurements could be made of its internal geometry.

## SECTION 4

### RESULTS

Nine different surfaces were tested. A total of twenty-three runs were made, most of them being with mirror finish plates. The large number of mirror finish runs were necessary in order to eliminate boiling from the "stress ring," to find the conditions for obtaining reproducible results, and to determine how various factors such as depth of liquid, number of data points and time interval between data points affected the  $Q/A$  vs  $(T_w - T_{sat})$  curves.

4.1 Natural Convection - Many of the data points taken were in the natural convection region. This was originally planned so that the experimenter could observe the boiling inception point.

It was later observed that the natural convection data did not fit the equations developed for horizontal flat plates (1) nor was it consistent from one run to another. Several exponents were calculated from the data plotted in Figures 12 through 19. They were found to vary from 1.1 to 1.45. Several reasons for this behavior may be postulated. First, the equations normally used for flat plates were developed using large sheets (about six feet long). The plates used in these tests were very small ( $2 \frac{3}{8}$  inch diameter) and were heated only in the center (one inch diameter). Natural convection correlations for small horizontal surfaces were not found in a literature search.

Secondly, two distinct types of convection modes were observed. Normally, the fluid seemed to sweep across the plate, first from one direction, then another. The heated liquid would then rise near the edge of the plate, and the process would begin again. In the second mode,

observed in only three of the runs, the liquid would sweep across the plate rising near the center. In this process the motion was not random - the liquid appeared to always travel in the same direction, producing a chimney effect. It would be expected that this second type would produce higher heat transfer coefficients due to the increased movement of liquid across the plate.

The third factor involved in the data scatter is the increased percentage of heat flux uncertainty in this region due to the very small temperature drop across the copper cylinder at low heat velocities.

It was noted on the curves containing a single cavity that there was a step increase in the heat flux as the inception point was approached. The natural convection data plotted in Figure 15 through 19 is approximated by a straight line. Figure 10 shows two curves plotted with this jump considered. There is presently no explanation for this phenomenon.

4.2 Hysteresis - Hysteresis is the effect of past heating history on the boiling curve. Several modes of hysteresis were observed in these experiments.

When a mirror finish surface was preboiled and cooled for fifteen minutes and then a run was made at a fast rate, a high degree of superheat could be achieved before the incipience of boiling. In this type of run the waiting time between data points was two to three minutes and very little time was spent in the natural convection region. The superheat would decrease upon a further increase in heat flux when at the incipient point. This phenomenon was also observed by Corty and Foust (4), Almgren and Smith (10) and others (12, 13, 17). Both Corty and Foust and Almgren and Smith explain this as being due to a lack of trapped vapor in the cavities of the surface. The extent of this



hysteresis was dependent on the amount of vapor trapped in the surface cavities.

When runs were made with the same specified preboiling, but with 45 minutes or more spent in the natural convection region, none of this type of hysteresis was observed.

A second type of hysteresis was noted after initiation of boiling. On increasing heat flux it was observed that if power input was held constant for a long period the temperature difference decreased. When decreasing heat flux the temperature difference increased. Figure 11 is a plot of two typical points showing their movement in detail. Figure 12 compares two runs made using the same surface but with different time intervals between points. The above hysteresis occurred at every data point. The maximum time spent at any point while observing this motion was 90 minutes. At that time very little movement could be seen.

Kosky (9) and others (10, 18) also noted this phenomenon on increasing heat flux. They attributed it to an increase in the number of active sites over the observation time period. Correspondingly, when the heat flux is decreased the extra sites formed at high heat fluxes slowly deactivate, causing the  $(T_w - T_{sat})$  to rise. As can be seen in Figure 11 the two points seem to converge toward one curve. Bonilla et al. (6) found that it took two hours or more for a point to become absolutely constant when testing with water.

The third type of hysteresis observed was: on descending heat flux curves, lower heat fluxes could be achieved while still maintaining active sites than when starting with no nucleating sites. The extreme cases were noted with the 0.015 inch mouth diameter cavities. This

hysteresis was due to there being present in the cavities vapor nuclei which continued to nucleate. Apparently very little superheat is required for a cavity of this size to nucleate once a vapor nucleus has been formed.

4.3 Reproducibility - Using the procedure outlined in the previous section, two mirror finish surfaces were run. The results are plotted in Figure 13. Although there is excellent agreement in the boiling region, there is a wide discrepancy in the natural convection curves. The mirror finish results in the boiling region are compared to Maynard's and Almgren and Smith's mirror finish results in Figure 14. Their surfaces were of the same material and approximately the same geometry. Differences in the curves can be seen but are slight. They are probably due to the use of different procedures. For example, Almgren and Smith took their data while decreasing flux, staying 45 minutes at each point.

4.4 Single Cylindrical Cavities - The data from the runs using single cylindrical cavities are plotted in Figure 15. In the natural convection region there is a large spread from one size cavity to another. It should be noted that the curves tended to move upward as cavity size increased. The 0.015 inch drilled hole had the highest heat transfer coefficients in this region while the mirror finish had the lowest. The size of cavities affected the natural convection data, probably by disturbance of the boundary layer.

Boiling inception occurred at essentially the same heat flux and temperature difference for all of these cavities. It occurred at about the same temperature difference as the mirror finish, but at a higher heat flux. This was contrary to the expected result, as predicted by Griffith and Wallis (5), that the larger cavities would activate at

lower temperature differences. Several reasons may be postulated to explain this observation. First, the artificial cavities may not have been the real active sites. That is, a smaller cavity may have existed within the holes. The bubbles growing from this smaller cavity would fill the larger cavity with vapor, thus, activating it. Secondly, as both Hsu (19) and Bergles and Rohsenow (20) point out, the thermal boundary layer thickness and fluid velocity play an important role in the size range of the active nucleation sites and consequently the superheat at boiling inception. Considering the natural convection patterns observed experimentally in this investigation (that is, increased heat transfer coefficients with artificial cavities, the sudden jump in heat transfer coefficient for some surfaces, and the intermittent "chimney effect") the thermal boundary layer thickness could have varied considerably, thus yielding the observed results.

Upon inception, for all but the smallest cavity (spark cut hole) the first bubble came from the hole and a patch developed around it. The patch, upon increasing heat flux, spread across the rest of the surface. From previous studies (5, 19) it was felt that large cavities (such as 0.015 inch diameter) would not activate first. Thus, upon completion of the run with the large hole, tests were conducted to determine if this cavity always activated first. It was found that the hole, under identical conditions, could be deactivated about 50% of the time.

In the nucleate boiling region, at the lower heat fluxes, the cavities appear to lower the temperature difference by about  $0.5^{\circ}\text{K}$ . The two curves then become closer, and at the final data point they are coincident. The slope of the curve for plates with cavities is lower than the slope of the mirror finish curve. This indicates that the

effect of the cavity on the boiling curve becomes less and less as more sites become active. The merging of the curves and the change in slope was also noted by several other authors (5, 6, 10, 12).

4.5 Conical Cavity - The 0.022 inch diameter conical cavity results are plotted in Figure 16 along with the single 0.015 inch cylinder and the mirror finish results. In this case, as above, the natural convection data for the larger cavity has the highest heat flux for a given temperature difference.

At the incipient point the conical hole did not activate first. A patch near the center of the plate spread over the hole and activated it. At incipience there was a very slight amount of hysteresis. Above the incipient point the conical cavity curve is to the left of both the mirror finish and the single 0.015 inch cylinder curves. This was expected since the conical cavity was larger than the cylinder (5). These curves converge at the upper limit of the data. As noted previously, these curves are not as steep as that for a mirror finish.

4.6 Multiple Spark Cut Holes - Figure 17 presents the results from the run with the 97 spark cut holes and compares it with the results from a single spark cut cavity.

The multiple cavity surface had higher heat transfer rates than the single cavity in the natural convection regime. Again this supports the idea that surface discontinuities affect heat transfer rates in this region.

As in the case of the single spark cut cavity, none of the 97 holes appeared to be activated prior to the development of a small boiling patch on the surface. The single cavity curve shows a  $0.5^{\circ}\text{K}$  lower temperature difference than for the 97 holes in the lower part of the

nucleate boiling curve. This was not expected. It is believed that the lack of depth and irregular shape of these holes (see Figure 8 and 9) have caused the data to be unreliable.

4.7 Multiple Drilled Holes - Two runs were made with each plate containing multiple holes. The first was to obtain data for plotting a  $Q/A$  vs temperature difference curve similar to those previously discussed. The second, with a fixed number of boiling artificial cavities, was to obtain data for plotting a  $Q/A$  vs temperature difference curve and to obtain data for determining an exponent for  $(n/A)$  in Yamagata's (22) equation,

$$Q/A = C_2 (\Delta T)^a (n/A)^b \quad (1)$$

where  $\Delta T$  is  $(T_w - T_{sat})$  and  $C_2$  is a constant.

The data from the first run with each plate is plotted on Figure 18 along with the data from the single 0.015 inch cylindrical cavity. Again, in the natural convection region an increase in the number of surface discontinuities increases the heat flux for a given temperature difference.

At the incipient point the temperature difference for multiple cavities was about  $0.75^\circ\text{K}$  lower than for the single cavity and the heat flux was considerably higher. This may have been due to the previously mentioned thermal boundary layer and fluid velocity changes that occurred with different surfaces. The plate with the largest number of cavities had the highest heat flux at incipience.

Boiling began from two artificial cavities on the plate with seven holes. Upon increasing the heat flux the five other holes began nucleating. Shortly thereafter a patch developed in the center of the plate.

A further increase in heat flux caused the patch to spread across the entire heated area. The plate with thirteen holes began nucleating from the center hole. An increase in heat flux started a small boiling patch around this hole and activated the other twelve artificial cavities. Upon a further increase in heat flux, the area including the inner seven holes, a circle of approximately 0.145 inch radius, boiled as a patch with the six outer holes also nucleating. Only during the last three data points in this run was there full boiling across the heated area (this also applies to the run with seven holes). For all other plates, at least the last five data points were for full boiling.

As noted previously the nucleate boiling curves converge as heat flux becomes high and the total number of active sites makes the effect of the few artificial cavities insignificant.

Figure 19 presents the data from the runs where a fixed number of cavities was active. On this curve is shown also the natural convection data obtained from these plates (dashed lines). It can be seen that the presence of the nucleating cavities has raised the heat flux for a given temperature difference. The amount of this rise increased with the number of active sites. It was observed that while there was a wide range of heat fluxes and temperature differences where one and seven cavities remained active, there was no point on the plate with thirteen holes where all thirteen cavities alone could be kept active. The point shown in Figure 19 is for ten active cavities. It was taken on a descending heat flux curve and it is not considered valid to compare this point to the other curves. Higher heat fluxes started patches boiling, lower fluxes deactivated some of the cavities. This particular surface was extensively dry sanded after the placement of the first seven holes

and again after the placement of the additional six holes, due to the presence of large burrs and scratches incurred in the drilling process. This regrinding may have had an effect on the boiling characteristics of the plate.

Yamagata and Nishikawa (22) proposed that

$$Q \propto \Delta T^a n^b \tag{2}$$

By fitting experimental data they found some values for a and b. Other experimenters (21, 23) modified some of the assumptions and the approach. They obtained different values for these exponents. A check on these values was made (Appendix C) using data from the one and seven active cavity runs. Table 4-1 compares these to the others that were obtained. The results are in good agreement with those previously obtained. Figure 20 is a plot of the data from these two runs and shows the curves obtained using the calculated exponents and constant. The equation used to plot both of the lines shown in Figure 20 was:

$$Q = 0.338 (\Delta T)^{1.36} (n)^{0.272} \tag{3}$$

TABLE 4 - 1

COMPARISON OF EXPONENTS FOR THE YAMAGATA EQUATION

<u>Author</u>	<u>Exponent "a"</u>	<u>Exponent "b"</u>
Moulson	1.36	0.272
Yamagata (22)	1.50	0.250
Zuber (23)	2.0	0.250
Tien (18)	1.0	0.500

## SECTION 5

### CONCLUSIONS AND RECOMMENDATIONS

The results lead to the following conclusions:

1. Artificial cavities affect the natural convection heat flux curve of liquid nitrogen.
2. 0.015 inch diameter cylindrical holes, larger cavities than previously expected, appear to remain active while boiling nitrogen.
3. Single cylindrical cavities of various sizes have the same effect on the boiling curve after incipience. The mirror finished surface heat transfer coefficient was raised by the same amount in each case.
4. Boiling heat flux in the isolated bubble region is proportional to the number of active sites raised to the 0.272 power.
5. The boiling curves for the surfaces tested merge toward the mirror finish boiling curve at high heat fluxes.



The following recommendations are made for future boiling investigations and equipment modification:

1. Study more intensively the effect of surface conditions on natural convection and the boiling inception point.
2. Continue the present studies with different size cavities and cavity densities. Cavity sizes between 0.004 and 0.015 inch diameter, and some larger than 15 thousandths inch diameter should be studied. Determine the maximum size a cylinder may reach and still remain active.
3. Investigate in more detail the boiling curves which can be obtained with fixed numbers of boiling cavities.
4. Study the effects of different cavity geometries (such as conical and reentrant) to determine which types of cavities remain active.
5. Enlarge the boiler can to permit easier assembly.
6. Change the thermocouples to glass-insulated types soldered into the boiler cylinders and connected to leads in the can with plugs.
7. Install plugs for all electrical connections in the boiler can.
8. Devise a method to prevent thermocouple leads from receiving heat from the heater or heater wires by conduction or radiation.

9. Lengthen the boiler cylinder and change the material to a type with lower thermal conductivity to allow installation of at least one more thermocouple and to give higher temperature drops across it in order to obtain more accurate results.

## BIBLIOGRAPHY

1. Giedt, W. H., "Principles of Engineering Heat Transfer," D. Van Nostrand Co., Princeton, N. J., (1957).
2. Berenson, P. J., "Transition Boiling Heat Transfer from a Horizontal Plate," NSF Technical Report Number 17, (1960).
3. Mead, B. R., Romie, F. E., and Guibert, A. G., "Liquid Superheat and Boiling Heat Transfer," Heat Trans. and Fluid Mech. Inst., Stanford Univ., Stanford Univ. Press, Stanford, Calif., (1951).
4. Corty, C. and Foust, A. S., "Surface Variables in Nucleate Boiling," Chem. Eng. Progress Symposium Series, St. Louis, (1953).
5. Griffith, P. and Wallis, J. D., "The Role of Surface Conditions in Nucleate Boiling," Chem. Eng. Progress Symposium Series, (1959).
6. Bonilla, C. F., Grady, J. J. and Avery, G. W., "Pool Boiling Heat Transfer from Scored Surfaces," Preprint 32, Sixth National Heat Transfer Conf., AIChE-ASME, Boston, Mass., (1963).
7. Class, C. R., Dettaan, J. R., Piccone, M., and Cost, R. B., "Boiling Heat Transfer to Liquid Hydrogen from Flat Surfaces," Paper E-5, Advances in Cryogenic Engineering, Vol. 5, Plenum Press, (1959).
8. Lyon, D. N., "Peak Nucleate Boiling Heat Fluxes and Nucleate Boiling Heat Transfer Coefficients for Liquid Nitrogen, Liquid Oxygen and their Mixtures in Pool Boiling at Atmospheric Pressures," Int J Heat Mass Transfer, Vol. 7, (1964), p 1097-1116.
9. Kosky, P. G., "Studies in Pool Boiling Heat Transfer to Cryogenic Liquids," Dissertation, Univ. of Calif., Berkeley, Calif., (1966).
10. Almgren, D. W. and Smith, J. L., "The Inception of Nucleate Boiling with Liquid Nitrogen," Document No. AFCRL-66-271, (1966).
11. Flynn, T. M., Draper, J. W. and Roos, J. J., "The Nucleate and Film Boiling of Liquid Nitrogen at One Atmosphere," Paper L-6, Advances in Cryogenic Engineering, Vol. 6, Plenum Press, (1960).
12. Maynard, M. D., "An Experimental Investigation of The Effects of Surface Conditions on Nucleate Pool Boiling Heat Transfer to Liquid Nitrogen from a Horizontal Surface," USNPGS M.S. Thesis, USNPGS, Monterey, Calif., (1966).
13. George, H. W., "An Experimental Investigation of Surface Effects on Nucleate Pool Boiling of Liquid Nitrogen from a Horizontal Surface," USNPGS M.S. Thesis, USNPGS, Monterey, Calif., (1967).

14. Rohsenow, W. M., "A Method of Correlating Heat Transfer," Trans. ASME, 74, (1952), p. 969-976.
15. Forster, K. and Zuber, N., "Growth of a Vapor Bubble in Superheated Liquid," J of Applied Phys., Vol. 25, (1958).
16. Baker, H. D., Ryder, E. A., and Baker, N. H., "Temperature Measurement in Engineering," John Wiley and Sons, New York, (1953).
17. Denny, V. E., "Some Effects of Surface Microgeometry on Natural Convection and Pool Boiling Heat Transfer to Saturated Carbon Tetrachloride," PhD Thesis, Univ. of Minn., (1961).
18. Marcus, B. D. and Dropkin, D., "Measured Temperature Profiles Within the Superheated Boundary Layer above a Horizontal Surface in Saturated Nucleate Pool Boiling of Water," Trans. ASME, Journal of Heat Transfer, Series C., Vol. 87, (1965), p. 333.
19. Hsu, Y. Y., "On the Size Range of Active Nucleation Cavities on Heating Surfaces," ASME Paper No. 61-WA-177, (1961).
20. Bergles, A. E., and Rohsenow, W. M., "Forced Convection Surface Boiling Heat Transfer and Burnout in Tubes of Small Diameter," Report No. 8767-21, ME Dept., M.I.T., (1962).
21. Tien, C. L., "A Hydrodynamic Model for Nucleate Pool Boiling," Int. J Heat Mass Transfer, Vol. 5, (1962), p. 533-540.
22. Yamagata, K. and Nishikawa, K., "On the Correlation of Nucleate Boiling Heat Transfer," Int. J Heat Mass Transfer, Vol. 1, (1960), p. 219-235.
23. Zuber, N., "Nucleate Boiling. The Region of Isolated Bubbles and the Similarity with Natural Convection," Int. J Heat Mass Transfer, Vol. 6, (1963), p. 53-68.
24. Powell, R. L., and Sparks, L. L., "Available Low Temperature Thermocouple Information and Services," NBS Report 8750, (1965).
25. Hodgman, C. D., "Handbook of Chemistry and Physics," Chemical Rubber Co., Cleveland, Ohio, 40th Ed., (1958).
26. Johnson, V. J. (ed), "A Compendium of the Properties of Materials at Low Temperatures," Phase II, December, (1961).

APPENDIX A  
THERMOCOUPLE CALIBRATION

Because a high degree of accuracy was desired, it was felt that all the components of the temperature measurement system should be thoroughly checked for reliability as well as accuracy. Direct instrument checking against secondary standards was chosen as the best means to achieve conveniently and cheaply the desired accuracy.

The measuring instrument used was a Leeds and Northrup K-3 Potentiometer. It was checked several times daily over a two week period with a standard cell of 1.01944 volts. No variation was ever noted. The instrument, when last calibrated by the manufacturer, was found to be accurate to within 0.2 microvolts, or 0.01% of the reading, whichever is larger.

Before calibrating the thermocouples, they were checked for reliability. This was accomplished by observing over a period of time the readings obtained using the ice-water equilibrium point as reference and inserting the thermocouples in boiling nitrogen. Readings were obtained over a five-day period during which seventeen observations were made. The difference between maximum and minimum readings for any thermocouple over this time span was 4.0 microvolts. Calibration of the thermocouples was then accomplished by using the following known points:

- (1) boiling nitrogen - melting ice
- (2) boiling argon - melting ice
- (3) boiling argon - boiling nitrogen.

The recorded emfs were the inputs to a computer program developed by NBS Cryogenic Laboratories at Boulder, Colo. (24). The program was purchased at cost from NBS by Maynard (12) who adapted it to Fortran 60 for use at

the Naval Postgraduate School. Due to a recent change in computers and computer language, this author converted the program to Fortran IV language. The program compared the spot calibration points to the NBS calibration table, computed a correction factor and then generated a working table for the range 0° to 300°K using any desired reference temperature in that range. A copy of the program and a sample working table are Appendix B. Each thermocouple was individually calibrated and a working table was obtained for each using the three calibration points (a total of fifteen working tables).

The tables constructed from the melting ice-boiling nitrogen data were chosen as the final working tables. The data was consistent and these were the points to be used in making the runs. Table A-1 is a summary of the calibration data. Table A-2 compares the calibration results. Figure 21 is a sample temperature versus emf curve made from this table. It was used in reducing the data.

TABLE A-1

THERMOCOUPLE CALIBRATION SUMMARY

<u>LN2 - ICE</u>		
<u>Thermocouple</u>	<u>EMF (<math>\mu</math>V)</u>	<u>Factor</u>
1	5486.1	0.99211
2	5487.2	0.99231
3	5487.4	0.99234
4	5487.1	0.99229
5	5487.2	0.99231
<u>LN2 - LA</u>		
1	167.9	0.99250
2	168.1	0.99368
3	168.7	0.99723
4	168.7	0.99723
5	168.5	0.99604
<u>LA - ICE</u>		
1	5320.9	0.99260
2	5321.2	0.99265
3	5320.4	0.99251
4	5321.3	0.99267
5	5321.2	0.99265

TABLE A-2

COMPARISON OF CALIBRATION DATALN<sub>2</sub> reference was used for this comparisonThermocouple #1

<u>Temp (°K)</u>	<u>LN<sub>2</sub>- ICE emf (μv)</u>	<u>LN<sub>2</sub>- LA emf (μv)</u>	<u>LA - ICE emf (μv)</u>	<u>MAX diff °K</u>
80	43.6	43.6	43.6	—
85	128.0	128.1	128.1	0.0063
90	215.9	216.0	216.0	0.0063
95	307.0	307.1	307.1	0.0063
100	401.4	401.6	401.6	0.0128

Thermocouple #2

80	43.6	43.7	43.6	0.0063
85	128.0	128.2	128.1	0.0125
90	216.0	216.3	216.0	0.019
95	307.1	307.5	307.2	0.025
100	401.5	402.1	401.7	0.038

Thermocouple #3

80	43.6	43.8	43.6	0.0125
85	128.0	128.7	128.1	0.044
90	216.0	217.0	216.0	0.063
95	307.1	308.6	307.1	0.094
100	401.5	403.5	401.6	0.125



Thermocouple #4

	LN2- ICE	LN2-LA	LA - ICE	Max Diff
<u>Temp (<math>^{\circ}</math>K)</u>	<u>emf</u>	<u>emf</u>	<u>emf</u>	<u><math>^{\circ}</math>K</u>
80	43.6	43.8	43.6	0.0125
85	128.0	128.1	128.1	0.044
90	216.0	217.0	216.0	0.063
95	307.0	308.6	307.2	0.094
100	401.5	403.5	401.7	0.125

Thermocouple #5

80	43.6	43.8	43.6	0.0125
85	128.0	128.5	128.1	0.031
90	216.0	216.8	216.0	0.050
95	307.1	308.2	307.2	0.068
100	401.5	403.0	401.7	0.094

APPENDIX B  
THERMOCOUPLE CALIBRATION PROGRAM

```

C FACTOR ADJUSTMENT OF PUBLISHED TABLES FOR UNITS, REF. TEMPS, AND FACTOR
C
C FIRST USER'S INPUT CARD
C COLUMN 1: PUT IN 1 FOR DEG K; OR 0 FOR DEG C
C COLUMN 2: PUT IN 1 FOR PUNCHED OUTPUT; PUT IN 2 FOR PRINTED OUTPUT
C COLUMNS 11-20: HIGH REFERENCE TEMPERATURE WITH DECIMAL POINT
C COLUMNS 21-30: LOW REFERENCE TEMPERATURE WITH DECIMAL POINT
C COLUMNS 31-40: OBSERVED EMF IN MICROVOLTS
C COLUMNS 41-50: DESIRED REFERENCE TEMPERATURE WITH DECIMAL POINT
C
C SECOND USER'S INPUT CARD
C COLUMNS 1-15: NAMES OF REFERENCE POINTS USED IN THE CALIBRATION
C COLUMNS 16-26: THERMOCOUPLE IDENTIFICATION NUMBER
C COLUMNS 27-42: USER'S NAME
C COLUMNS 43-64: DATE OF CALIBRATION
C
C THIRD USER'S CARD- MUST PRECEED SUBSEQUENT (AND ALL OTHER) FIRST
C AND SECOND USER'S INPUT CARDS WHEN MULTIPLE TABLE OUTPUT IS DESIRED.
C COLUMNS 1-21: REPEAT LAST T. C. DECK
C COLUMN 50: 0 (ZFRQ)
C COLUMNS 55-60: DEG. K
C COLUMNS 68-70: YES
C
C IMPLICIT REAL*8(A-H), REAL*9(I-Z)
C 90 DIMENSION T(300), IT(300), IOC(300), EMFIN(300), EMF(300), DELEM(300),
C 91 DEDTIN(300), DEDT(300)
C 10 FORMAT(11,11,8X,4F10.0)
C 11 FORMAT(49X,11,4X,2A4,5X,A3)
C 12 FORMAT(A6,A6,A6,A3,5X,A6,4X,A6,8X,A6,A6,A2)
C 13 FORMAT(A6,A4,F10.0,F10.2,F10.3,10X,F10.0,F10.2,F10.3)
C 14 FORMAT(10X,3I10,4A6,A2)
C 16 FORMAT(2(13X,3F10.0))
C 30 FORMAT(3X,4HTEMP,5X,3HEMF,3X,6HDELEMF,5X,5HDE/DT,7X,4HTEMP,5X,
C 3013HEMF,3X,6HDELEMF,5X,5HDE/DT,3X)
C 40 FORMAT(2X,5HDEG K,4X,5HMIC V,2X,5HMIC V/DGK//)
C 4014X,5HMIC V,2X,5HMIC V,4X,9HMIC V,2X,5HMIC V/DGK//)
C 4114X,5HMIC V,2X,5HMIC V,4X,9HMIC V,2X,5HMIC V/DGK//)
C 50 FORMAT(17,F10.2,F7.2,F10.3,I11,F10.1,F7.1,F10.3//)
C 55 FORMAT(17,F10.2,F7.2,F10.3,I11,F10.1,F7.1,F10.3)
C 60 FORMAT(17,F9.1,F7.1,F11.3,I11,F10.1,F7.1,F10.3//)
C 65 FORMAT(17,F9.1,F7.1,F11.3,I11,F10.1,F7.1,F10.3)
C 70 FORMAT(17,F9.1,F7.1,F11.3//)
C 80 FORMAT(1H1,24H THERMOCOUPLE TABLE FOR ,A6,4H VS ,A6,11H, ISA TYPE
C 801,A6,A2,10H, BASED ON/29H NAT. BUR. OF STANDARDS PUB. ,A6,28H WITH
C 802,CALC. MULT. FACTOR OF ,F7.5,1H./1X,A6,A6,A3,6H, LOT ,A6,29H. USERS

```

803 REFERENCE TEMPERATURE,F7.3,IX,A6/16X,10HTEST DATE ,A6,A6,A2,5H B  
 804Y ,A6,A6//)

C DATA DECK AND KEY CARDS READ IN  
 100 READ (5,11) IA,ATEST1,ATEST2  
 102 IF (IA) 140,140,105

105 READ (5,14) ITEMP1,ITABLE,IFMTCH,AMATP,AMATN,APIB,  
 1051 ATYPE1,ATYPE2  
 110 K2=IFMTCH+1  
 112 ITEMPL=ITABLE  
 115 DO 130 I=ITEMPI,ITEMPL,2  
 120 READ (5,16) T(I),EMFIN(I),DEDTIN(I),T(I+1),EMFIN(I+1),  
 1201 DEDTIN(I+1)  
 130 CONTINUE

132 K9=K2  
 133 IF (IFMTCH) 134,134,140  
 134 K9=K2+1  
 140 READ(5,10)KKK,ICAR ,TEMPHI,TEMPLO,ETEST,UREFT  
 141 ITABLE=ITEMPL  
 142 IUNIT=1  
 144 REFTMP=UREFT  
 150 READ (5,12) ACOMP1,ACOMP2,ACOMP3,ALOT,ANAME1,ANAMEL,  
 1501ADATE1,ADATE2,ADATE3

C CONVERSION OF REFTMP,TEMPHI, AND TEMPLO INTO DEG. K SYSTEM

151 IF (KKK-1) 152,152,152  
 152 REFTMP=REFTMP+273.15  
 152 TEMPHI=TEMPHI+273.15  
 152 TEMPLO=TEMPLO+273.15  
 3152 IUNIT=2

C COMPUTATION OF FACTOR

155 ITEMPLO=TEMPLO  
 160 TEMP3=ITEMPLO-1  
 165 TEMP4=ITEMPLO  
 170 TEMP5=ITEMPLO+ITEMPLO-1  
 180 EMF13=EMFIN(ITEMPLO)  
 185 EMF15=EMFIN(ITEMPLO+1)  
 190 V=EMF13\*((TEMPLO-TEMP4))\*((TEMPLO-TEMP5)/2.0  
 195 W=EMF14\*((TEMPLO-TEMP3))\*((TEMPLO-TEMP4)/2.0  
 200 EMFLO=U+V+W  
 205 ITEMPHI=TEMPHI  
 210 ITEMP6=ITEMPHI-1  
 220 ITEMP7=ITEMPHI  
 225 ITEMP8=ITEMPHI+1  
 230 EMF16=EMFIN(ITEMPHI-1)

```

235 EMFI7=EMFIN(I,TEMPHI)
240 EMFI8=EMFIN(I,TEMPHI+1)
245 X=EMFI6*(TEMPHI-TEMP7)*((TEMPHI-TEMP8)/2.0)
250 Y=EMFI7*(TEMPHI-TEMP6)*((TEMPHI-TEMP7)/2.0)
255 Z=EMFI8*(TEMPHI-TEMP6)*((TEMPHI-TEMP7)/2.0)
260 EMFHI=X+Y+Z
265 ETABLE=EMFHI-EMFLO
270 FACTOR=ETEST/ETABLE

```

C

```

CALCULATION OF EMFR
305 IF(REFTMP) 320,310,320
310 EMFR=0.0
315 GO TO 375
320 ITEMPC=REFTMP
325 ITEMP0=ITEMPO
330 TEMP1=TEMP0+1.0
335 TEMP2=TEMP0+2.0
340 EMF10=EMFIN(ITEMPO)
345 EMF11=EMFIN(ITEMPO+1)
350 EMF12=EMFIN(ITEMPO+2)
355 A=EMF10*((REFTMP-TEMP1)*((REFTMP-TEMP2)/2.0)
360 B=EMF11*((REFTMP-TEMP0)*((TEMP2-REFTMP)
365 C=EMF12*((REFTMP-TEMP0)*((REFTMP-TEMP1)/2.0)
372 EMFR=(A+B+C)*FACTOR
374 IF(IUNIT-1)465,375,465

```

C

```

CALCULATION OF EMF AND DEDT FOR ENTIRE TEMP. RANGE
375 DO 395 J=I,TEMP1,ITEMPL
380 Y(J)=Y(J)
385 EMF(J)=EMFIN(J)*FACTOR-EMFR
390 DEDT(J)=DEDTIN(J)*FACTOR
395 CONTINUE
396 GO TO 398

```

C

```

EMF, DELEMF, AND DEDT VALUES CORRESPONDING TO EVEN DEG. C
465 K3=ITEMPL-2
470 DO 540 I=ITEMPI,K3
480 D=EMFIN(I)*0.78625
485 E=EMFIN(I+1)*0.27750
490 F=EMFIN(I+2)*(-0.06375)
495 EMF(I)=(D+E+F)*FACTOR-EMFR
500 X=DEDTIN(I)*0.78625
505 Y=DEDTIN(I+1)*0.27750
510 Z=DEDTIN(I+2)*(-0.06375)
515 DEDTTI)=(X+Y+Z)*FACTOR
540 CONTINUE
545 K4=K3+1
560 D1=EMFIN(K4-1)*(-0.06375)

```

```

565 E1=EMFIN(K4)*C.97750
570 F1=EMFIN(K4+1)*0.08625
575 EMF(K4)=(D1+F1+F1)*FACTOR-EMFR
580 X1=DEDIIN(K4-L)*(-0.06375)
585 Y1=DEDIIN(K4)*C.97750
590 Z1=DEDIIN(K4+1)*0.08625
595 DEDT(K4)=(X1+Y1+Z1)*FACTOR
620 ITABLE=ITABLE-I
625 DO 635 I=ITEMPI,273
630 IT(I)=T(I)-273.15
635 CONTINUE
640 DO 650 I=274,ITABLE
645 IT(I)=T(I)-272.85
650 CONTINUE

```

C  
C

```

CALCULATION OF DELEMF
398 DELEM(I)=EMF(I)+EMFR
399 LI=ITEMPI+1
400 DO 420 J=LI,IFMTCH
405 E2=EMF(J)+0.005
410 E3=EMF(J-1)+0.005
415 DELEM(J)=EMF(J)-EMF(J-1)-DMOD(E2,0.01D0)+DMOD(E3,0.01D0)
420 CONTINUE
425 DO 445 J=K9,ITABLE
430 E4=EMF(J)+0.05
435 E5=EMF(J-1)+0.05
440 DELEM(J)=EMF(J)-EMF(J-1)-DMOD(E4,0.1D0)+DMOD(E5,.1D0)
445 CONTINUE

```

C  
C

```

PAGE HEADING WRITEOUT
665 WRITE(6,80) AMATP,AMATN,AJYPE1,ATYPE2,APUB,FACTOR,
6652 ANAME1,ANAMEL
680 WRITE(6,30)
685 GO TO(690,700),IUNIT
690 WRITE(6,40)
695 GO TO 704
700 WRITE(6,41)

```

C  
C

```

WRITEOUT FOR PARAMETERS FROM T=1 TO T=FORMAT CHANGE
704 IF(IFMTCH)780,780,705
705 DO 775 L=ITEMPI,IFMTCH
710 IF( MOD(L-ITEMPI+1,5))735,715,735
715 IF( MOD(L-ITEMPI+1,40))735,735,725
725 WRITE(6,50) IT(L),EMF(L),DELT(L),IT(L+40),
7251EMF(L+40),DELEM(L+40),DELT(L+40)
730 GO TO 775
735 WRITE(6,55)IT(L),EMF(L),DELEM(L),DELT(L),IT(L+40),

```

```

7351EMF(L+40),DELFM(L+4C),DEDT(L+40)
775 CONTINUE
C
WRITE OUT FOR PARAMETERS FROM I=FORMAT CHANGE TO I=4C
800 DO 850 L=K2,40
785 IF (MOD(L-IITEMPI+1,5))810,790,810
790 IF (MOD(L-IITEMPI+1,40))810,810,800
800 WRITE(6,60)IT(L),EMF(L),DELEM(L),DEDT(L),IT(L+40),
8001EMF(L+40),DELEM(L+40),DEDT(L+40)
805 GO TO 850
810 WRITE(6,65)IT(L),EMF(L),DELEM(L),DEDT(L),IT(L+40),
8101EMF(L+40),DELEM(L+4C),DEDT(L+40)
850 CONTINUE
855 N=C
C
PAGE HEADING WRITE OUT
865 WRITE(6,80)AMATP,AMATN,ATYPE1,ATYPE2,APUB,FACTOR,
8651ACOMP1,ACOMP2,ACOMP3,ALOT,URFFT,AUNIT,ADATE1,ADATE2,ADATE3,
8652ANAME1,ANAMEL
870 WRITE(6,30)
875 GO TO (880,890),IUNIT
880 WRITE(6,40)
885 GO TO 900
890 WRITE(6,41)
C
PARAMETER WRITE OUT FOR SECOND, THIRD, ETC. PAGES
900 N=N+1
905 J=80*N+1
906 JE=J+39
910 DO 1065 L=J,JE
930 IF (L-IITABLE)935,935,1075
935 IF (L+40-IITABLE)940,940,1005
940 IF (MOD(L-IITEMPI+1,5))965,945,965
945 IF (MOD(L-IITEMPI+1,40))965,965,955
955 WRITE(6,60)IT(L),EMF(L),DELEM(L),DEDT(L),IT(L+40),
9551EMF(L+40),DELEM(L+40),DEDT(L+40)
960 GO TO 1065
965 WRITE(6,65)IT(L),EMF(L),DELEM(L),DEDT(L),IT(L+40),
9651EMF(L+40),DELEM(L+40),DEDT(L+40)
970 GO TO 1065
1005 IF (MOD(L-IITEMPI+1,5))1030,1010,1030
1010 IF (MOD(L-IITEMPI+1,40))1030,1030,1020
1020 WRITE(6,70)IT(L),EMF(L),DELEM(L),DEDT(L)
1025 GO TO 1065
1030 WRITE(6,65)IT(L),EMF(L),DELEM(L),DEDT(L)
1065 CONTINUE
1070 IF (J+79-IITABLE)865,1075,1075

```

```

: C      PUNCHED DECK OUTPUT
1075 IF (ICAR-1) 1200, 1080, 1200
1080 CONTINUE
      DO 1100 I=1, IEMPI, 1TABLE, 2
1085   TOC(I) = IT(I)
1090   TOC(I+1) = IT(I+1)
1091 IF (I-I*TABLE) 1095, 1097, 1097
1095 WRITE(7, 13) AMATP, AMATN, TOC(I), EMF(I), DEDT(I), TOC(I+1),
1096 EMF(I+1), DEDT(I+1)
1096 GO TO 1100
1097 WRITE(7, 13) AMATP, AMATN, TOC(I), EMF(I), DEDT(I)
1100 CONTINUE
1500 WRITE(6, 1500)
1200 FORMAT(1H1)
1200 GO TO 100
      END

```

TABLE B-1

THERMOCOUPLE DATA

THERMOCOUPLE TABLE FOR COPPER VS CONST. CALC. ISA TYPE TP-IN BASED ON  
 NAT. BUR. OF STANDARDS PUB. R-188 WITH MULT. FACTOR OF 0.99231.  
 LN2-ICE CALIB. LOT NO 2. USERS REFERENCE TEMPERATURE 77.340  
 TEST DATE 3 AUGUST 1967 BY MOULSON

TEMP DEG K	EMF MIC V	DELEMF MIC V	DE/DT MIC V/DGK	TEMP DEG K	EMF MIC V	DELEMF MIC V	DE/DT MIC V/DGK
81	60.2	16.6	16.716	121	832.9	21.9	21.858
82	76.9	16.7	16.848	122	854.8	21.9	21.983
83	93.8	16.9	16.980	123	876.8	22.0	22.108
84	110.9	17.1	17.112	124	899.0	22.2	22.233
85	128.0	17.1	17.244	125	921.3	22.3	22.357
86	145.3	17.3	17.376	126	943.7	22.4	22.481
87	162.8	17.5	17.508	127	966.2	22.5	22.605
88	180.3	17.5	17.640	128	988.9	22.7	22.729
89	198.1	17.8	17.772	129	1011.7	22.8	22.853
90	216.0	17.9	17.904	130	1034.6	22.9	22.977
91	233.9	17.9	18.036	131	1057.6	23.0	23.102
92	252.0	18.1	18.168	132	1080.9	23.3	23.227
93	270.2	18.2	18.299	133	1104.2	23.3	23.352
94	288.6	18.4	18.430	134	1127.6	23.4	23.477
95	307.1	18.5	18.561	135	1151.1	23.5	23.601
96	325.7	18.6	18.691	136	1174.7	23.6	23.726
97	344.5	18.8	18.821	137	1198.5	23.8	23.851
98	363.3	18.8	18.950	138	1222.5	24.0	23.976
99	382.4	19.1	19.079	139	1246.5	24.0	24.101
100	401.5	19.1	19.208	140	1270.6	24.1	24.226
101	420.8	19.3	19.336	141	1294.9	24.3	24.351
102	440.2	19.4	19.464	142	1319.3	24.4	24.476
103	459.8	19.6	19.592	143	1343.8	24.5	24.602
104	479.4	19.6	19.720	144	1368.5	24.7	24.727
105	499.2	19.8	19.847	145	1393.3	24.8	24.852



## APPENDIX C

### SAMPLE CALCULATION WITH ERROR ANALYSIS

#### Assumptions

1. The liquid nitrogen and ice used in calibration were of the same purity as that used in runs.
2. The effective thermocouple junction positions were known to  $\pm 0.010$  inches due to uncertainty in location of the junction in the sheathing and  $\pm 0.003$  inches uncertainty in location of thermocouple hole.
3. Barometric Pressure was accurate to  $\pm 0.05$  mm Hg.
4. Thermal conductivities of copper were within 5% of the reference curve (Figure 22).
5. Measured nitrogen depths were accurate to within 0.2 centimeters.
6. Thermocouple working tables accurate to  $\pm 0.1 \mu\text{V}$ ; thermocouple readings accurate to  $\pm 0.1 \mu\text{V}$  and thermocouples reliable to  $\pm 4.0 \mu\text{V}$ , or a maximum uncertainty of  $4.2 \mu\text{V}$  per reading.
7. The objective of the error analysis was to determine the probable error in the results.

The data used is from point eleven of run thirteen (0.0043 in. dia. cylindrical hole).

TABLE C-1

THERMOCOUPLE DATA

<u>T. C.</u>	<u>Location (inches)</u>	<u>Location (cm)</u>	<u>Temp (<math>^{\circ}\text{K}</math>)</u>
1	$0.684 \pm 0.010$	$1.735 \pm 0.027$	$84.11 \pm .24$
2	$0.534 \pm 0.010$	$1.360 \pm 0.027$	$83.70 \pm .25$
3	$0.384 \pm 0.010$	$0.975 \pm 0.027$	$83.36 \pm .25$
4	$0.204 \pm 0.010$	$0.519 \pm 0.027$	$82.97 \pm .25$

## Surface Temperature and Heat Flux

In order to determine heat flux and surface temperature, the temperatures of the four thermocouples were plotted against distance from the boiling surface. The Fourier heat conduction law governs this situation: since this was a steady state conduction problem, a linear plot of temperature vs distance was expected and observed.

$$Q/A = k \frac{dT}{dx} \quad (C-1)$$

Figure 23 is a plot of the four temperatures listed in Table C-1 versus distance from the surface. The best line was determined by the eyeballing method. The surface temperature was determined by extrapolating this line to the vertical axis. Error limits showing the maximum uncertainties in temperature and distance are shown on this plot.

The most probable error in a single data point in Figure 23 is considered to be less than the maximum error limits shown, especially in the temperature measurements. The reason for this is that the error limits for temperature were derived from observing thermocouple reading variations over a long period of time and recording their fluctuations. The fluctuations were slow, with minimum and maximum readings occurring 12-20 hours apart and, they appeared to be more or less ambient temperature dependent.

From observing the deviations in this plot and others similar to it, the author considers reasonable a probable uncertainty of  $\pm 0.1^\circ\text{K}$ , shown as the shaded area about each data point in Figure 23.

By drawing straight lines through the extremes of these error boxes, an estimate of the most probable error was made. The results are shown in Table C-2.

TABLE C-2

SUMMARY OF ERROR DATA

<u>Tw (°K)</u>		<u>dT/dx</u>
82.50	BEST	0.94
82.65	MAX	1.06
82.34	MIN	0.81

This may be expressed as:  $T_w = 82.50 \pm .15^\circ\text{K}$  and  $dT/dx = 0.94 \pm .13 \text{ }^\circ\text{K/cm}$ .

For the determination of heat flux error, the following was used:

$$\begin{aligned}
 Q/A &= k \, dT/dx \\
 &= (5.11)(.94) \\
 &= 4.80 \text{ watts/cm}^2 \\
 \log(Q/A) &= \log(k) + \log(dT/dx) \\
 \frac{d(Q/A)}{Q/A} &= \frac{d(k)}{k} + \frac{d(dT/dx)}{dT/dx} \quad (C-2)
 \end{aligned}$$

For the root mean square error:

$$\frac{\Delta(Q/A)}{Q/A} = \sqrt{\left[\frac{\Delta k}{k}\right]^2 + \left[\frac{\Delta dT/dx}{dT/dx}\right]^2} \quad (C-3)$$

Substituting,

$$\frac{\Delta(Q/A)}{Q/A} = \sqrt{(.05)^2 + \left(\frac{.13}{.94}\right)^2}$$

or,

$$\frac{\Delta(Q/A)}{Q/A} = 0.1475$$

$$Q/A = 4.80 \pm 0.709 \text{ watts/cm}^2$$

### Saturation Temperature

The depth of nitrogen above the boiler surface was kept between 12 and 16 centimeters. An average of 14 cm was used for determining static pressure head.

$$\begin{aligned} P_{\text{HEAD}} &= \gamma H & (C-4) \\ &= (50.4) \left( \frac{14 \pm 2}{2.54} \right) \left( \frac{1}{1728} \right) \left( \frac{760}{14.696} \right) \\ &= 8.32 \pm 1.19 \text{ mm Hg} \\ \Delta P_{\text{ATM}} &= 762.3 \pm .05 - 760 \text{ mm Hg} \\ \Delta P_{\text{TOT}} &= P_{\text{HEAD}} + \Delta P_{\text{ATM}} \\ &= 10.62 \pm 1.24 \text{ mm Hg} \end{aligned}$$

From Reference 25, the following correction should be made:

$$T = 77.347 + .0109 P_{\text{TOT}} \quad (C-5)$$

thus,

$$T = 77.347 + (.0109)(10.62) \pm (1.24)(.0109)$$

$$T = 77.463 \pm 0.0135 \text{ } ^\circ\text{K}$$

### Temperature Difference

$$\Delta T = T_w - T_{\text{SAT}} \quad (C-6)$$

$$\Delta T = 82.50 - 77.46 \pm \sqrt{(.013)^2 + (.15)^2}$$

$$\Delta T = 5.04 \pm 0.15 \text{ } ^\circ\text{K}$$

## Natural Convection

Ref (1) states that in natural convection the heat flux is proportional to the temperature difference,  $T_w - T_{\text{bulk}}$ , raised to the 1.25 - 1.33 power, depending on presence of turbulence. Assuming that after pre-boiling, the saturation temperature is equal to the bulk temperature, then

$$\Delta T = T_w - T_{\text{BULK}}$$

$$= T_w - T_{\text{SAT}}$$

$$Q/A = C, \Delta T^x \quad (\text{C-7})$$

$$\frac{(Q/A)_1}{(Q/A)_2} = \frac{(\Delta T)_1^x}{(\Delta T)_2^x} \quad (\text{C-8})$$

From Run 14, two points in the natural convection region were chosen:

$$\log (Q/A)_1 - \log (Q/A)_2 = x [ \log (\Delta T)_1 - \log (\Delta T)_2 ]$$

$$x = \frac{\log (Q/A)_1 - \log (Q/A)_2}{\log (\Delta T)_1 - \log (\Delta T)_2}$$

$$= \frac{\log (.482) - \log (1.555)}{\log (1.70) - \log (4.13)}$$

$$= 1.35$$

Exponent of n/A

Yamagata and Nishikawa proposed:

$$Q \propto \Delta T^a n^b \quad (C-9)$$

where  $\Delta T$  is  $(T_w - T_{sat})$ . A check on the values of  $a$  and  $b$  is calculated below. The data used is from Figure 18.

$$\frac{(Q/A)_1}{(Q/A)_2} = \frac{(C_2)(\Delta T_1)^a (n_1)^b}{(C_2)(\Delta T_2)^a (n_2)^b} \quad (C-10)$$

From the curve with a single active cavity:

$$\frac{(Q/A)_1}{(Q/A)_2} = \frac{(\Delta T)_1^a}{(\Delta T)_2^a}$$

$$\frac{.34}{1.52} = \frac{1}{3^a}$$
$$a = 1.36$$

at constant  $\Delta T$ :

$$\frac{(Q/A)_1}{(Q/A)_2} = \frac{(n_1)^b}{(n_2)^b}$$

$$\frac{1.5}{2.55} = \left(\frac{1}{7}\right)^b$$

$$b = 0.272$$

and,

$$Q/A = C_2 \Delta T^a n^b$$

thus,

$$2.55 = C_2 (3.0)^{1.36} (7)^{0.272}$$

or

$$C_2 = 0.338$$

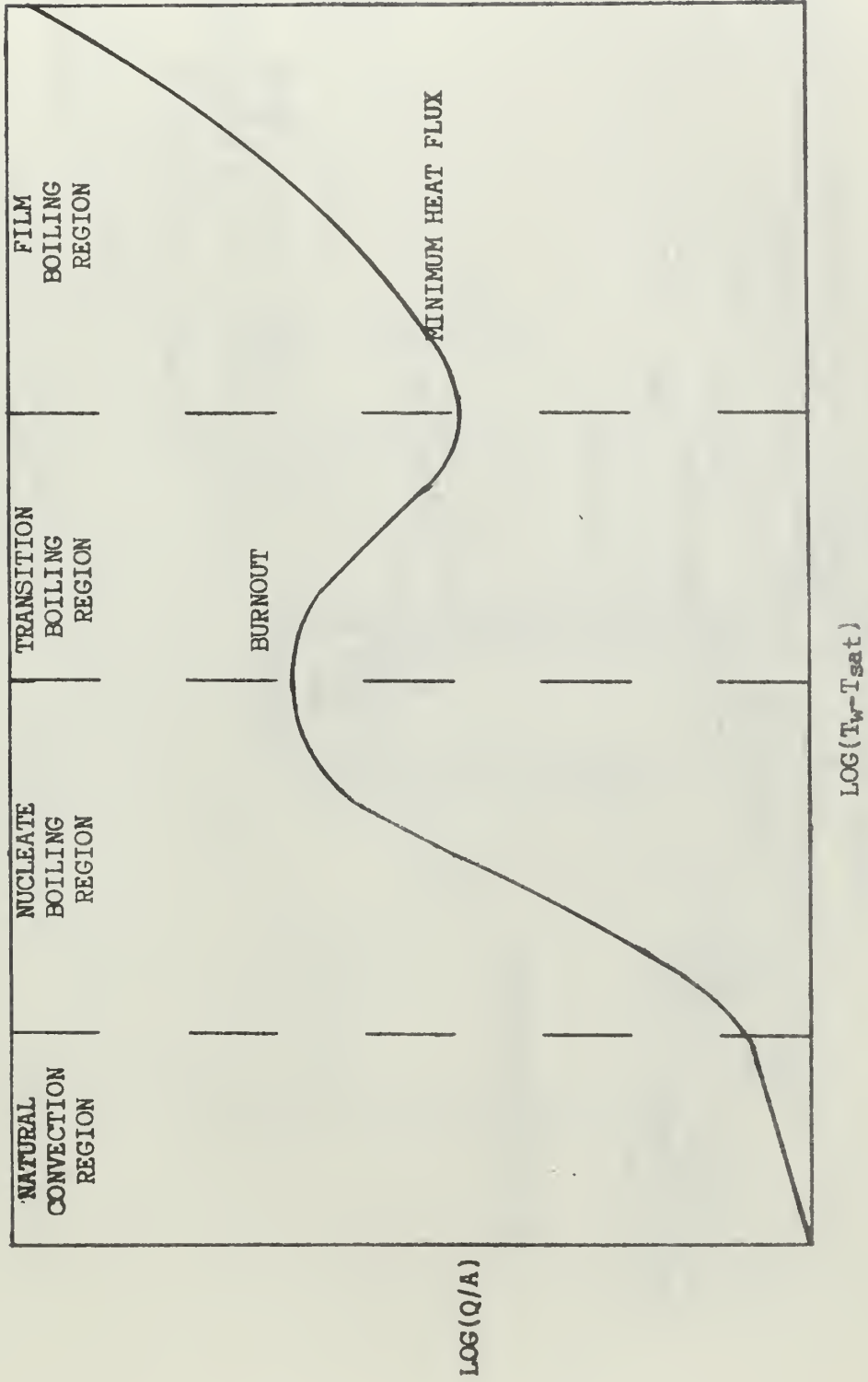


FIGURE 1. CHARACTERISTIC BOILING CURVE

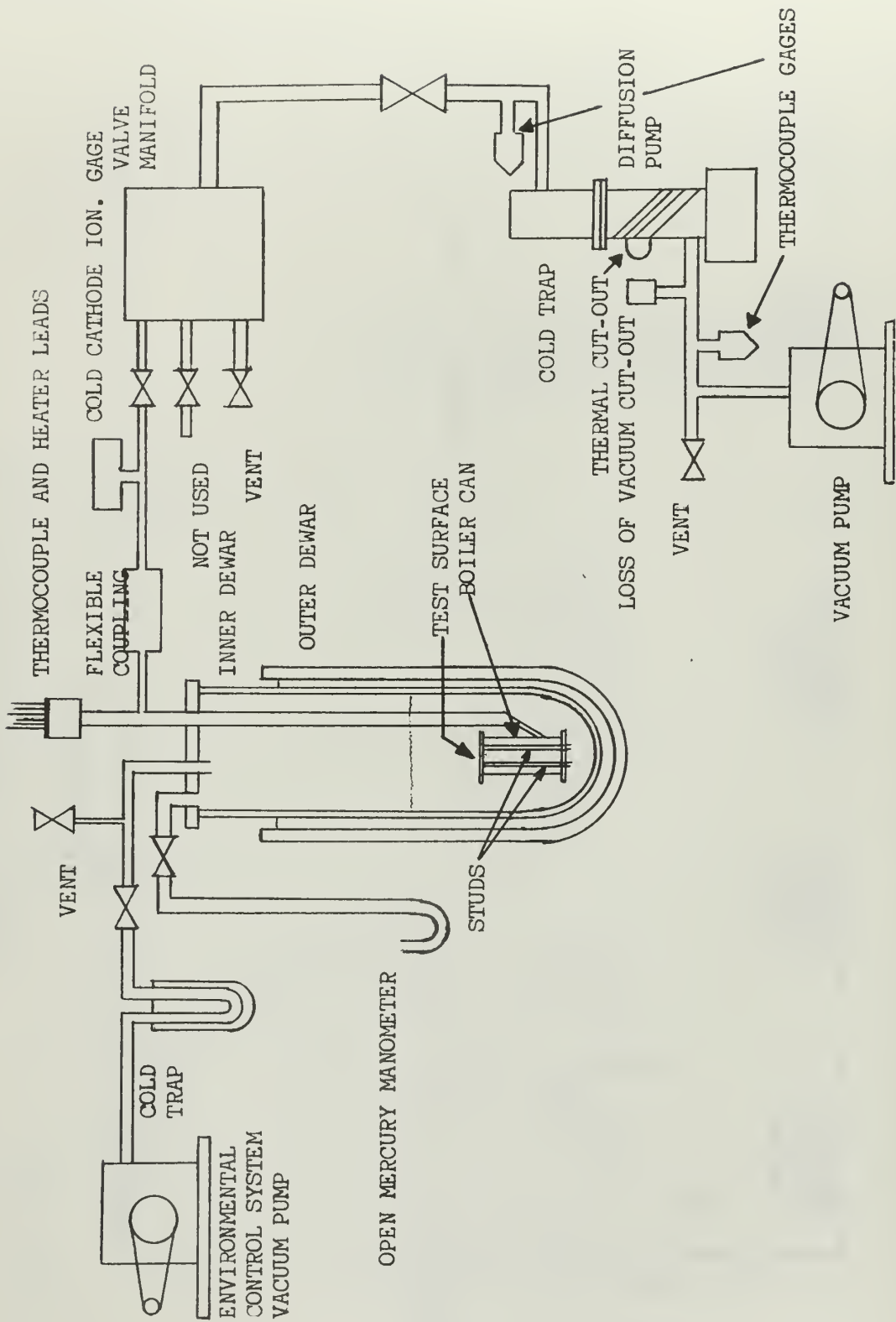


FIGURE 2. SCHEMATIC OF SYSTEM



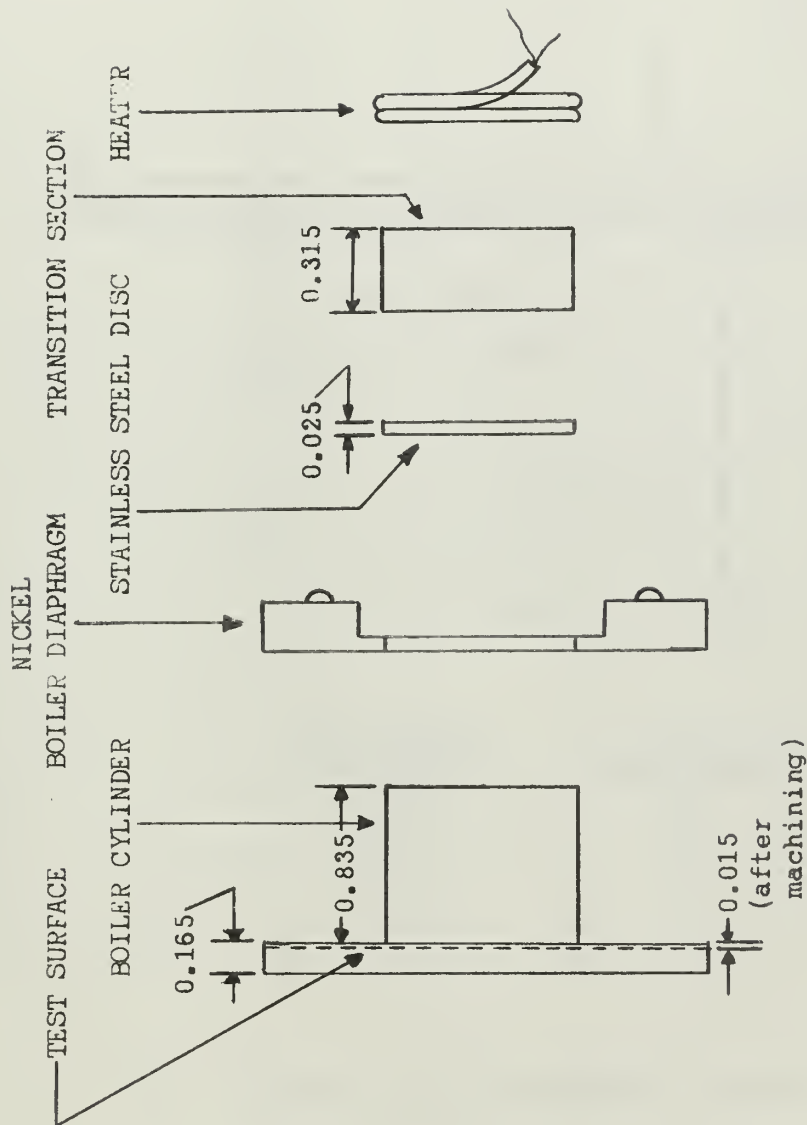
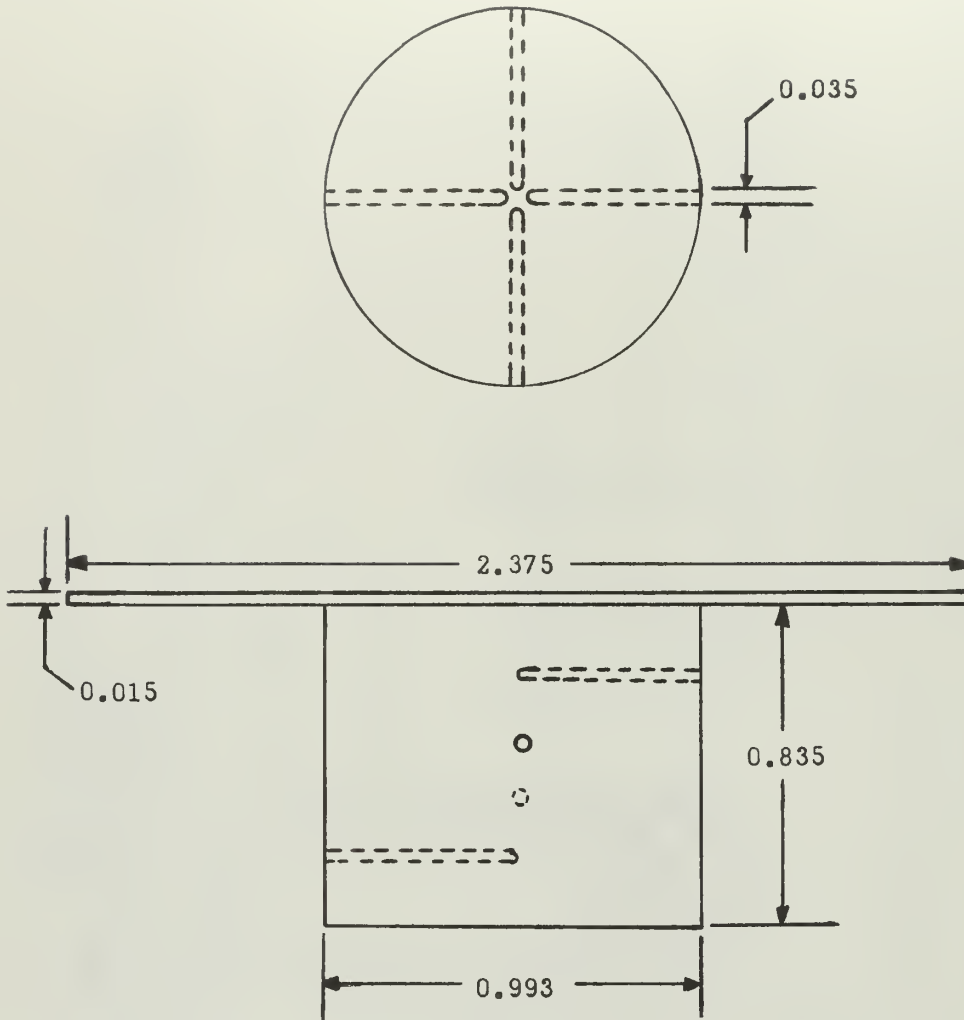


FIGURE 3. TEST SURFACE ASSEMBLY



<u>THERMOCOUPLE</u>	<u>DISTANCE TO TEST SURFACE</u>
1	0.684
2	0.534
3	0.384
4	0.204

FIGURE 4. THERMOCOUPLE WELL LOCATIONS

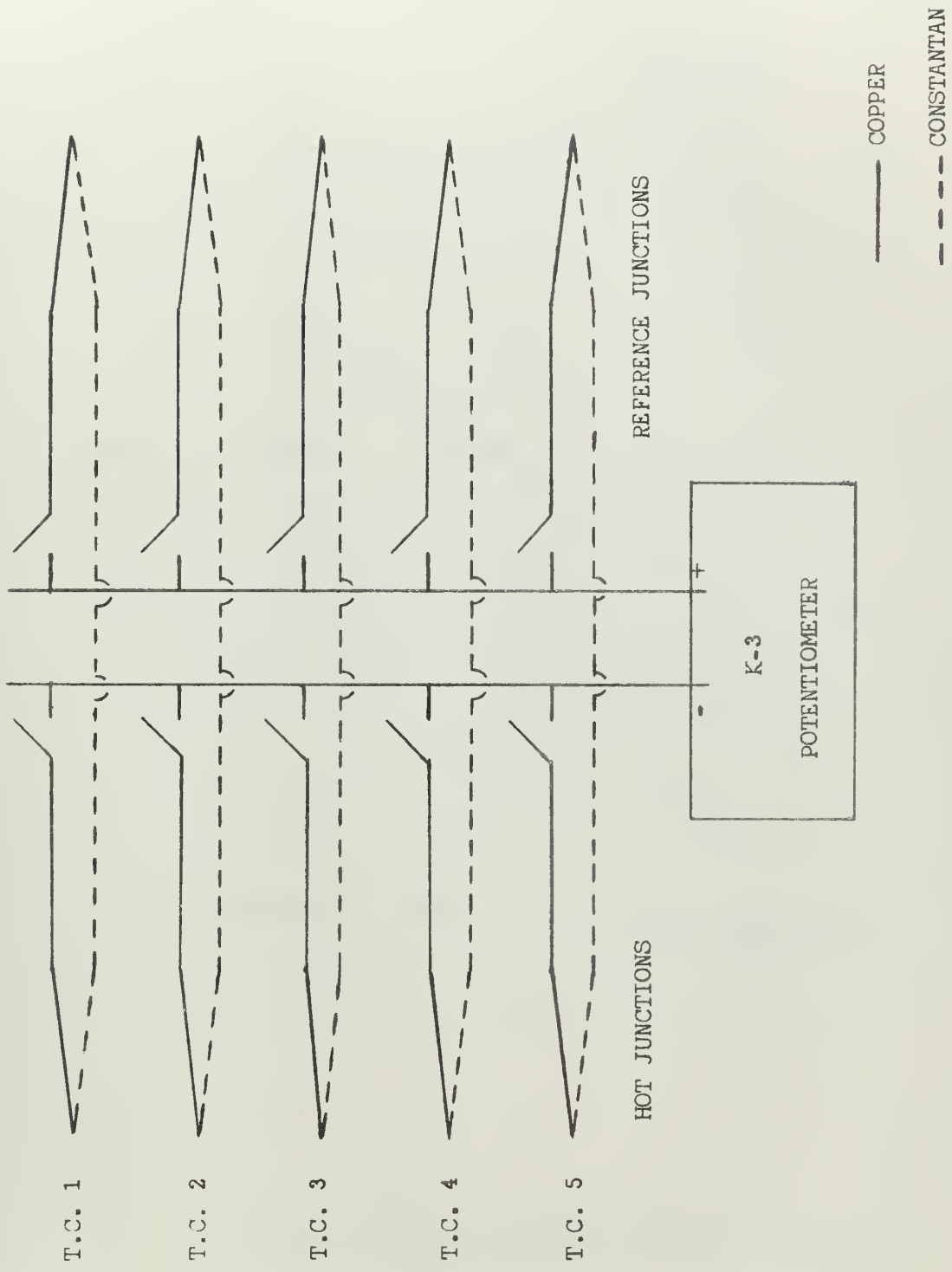
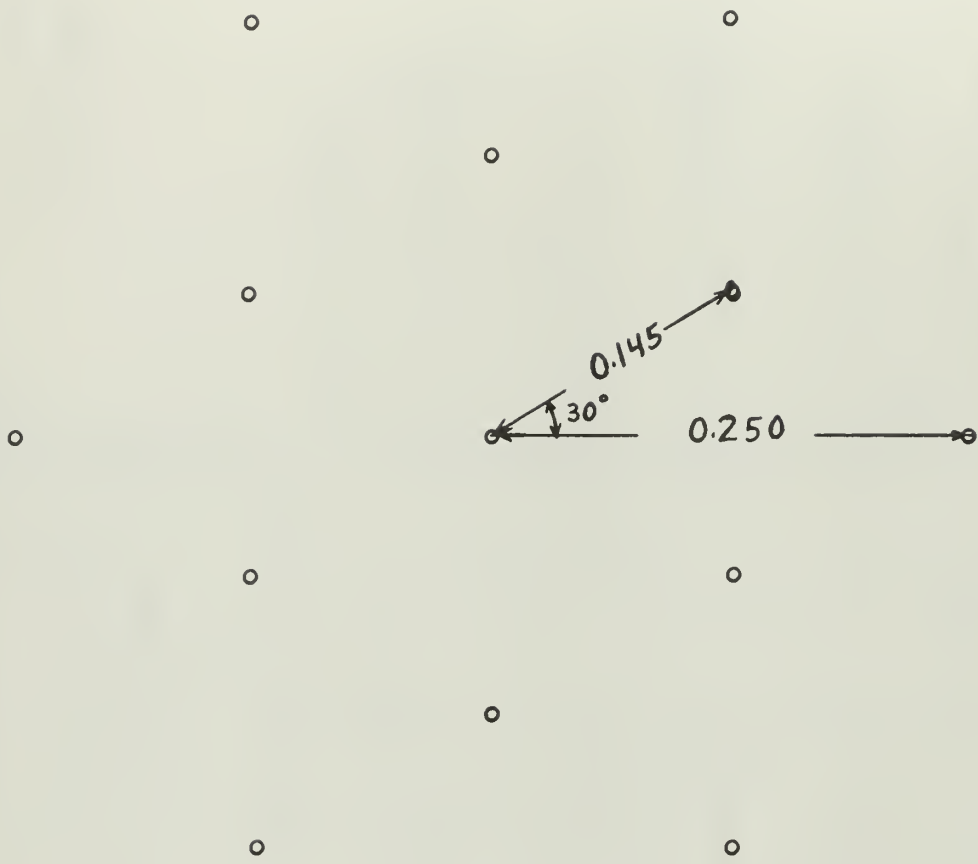
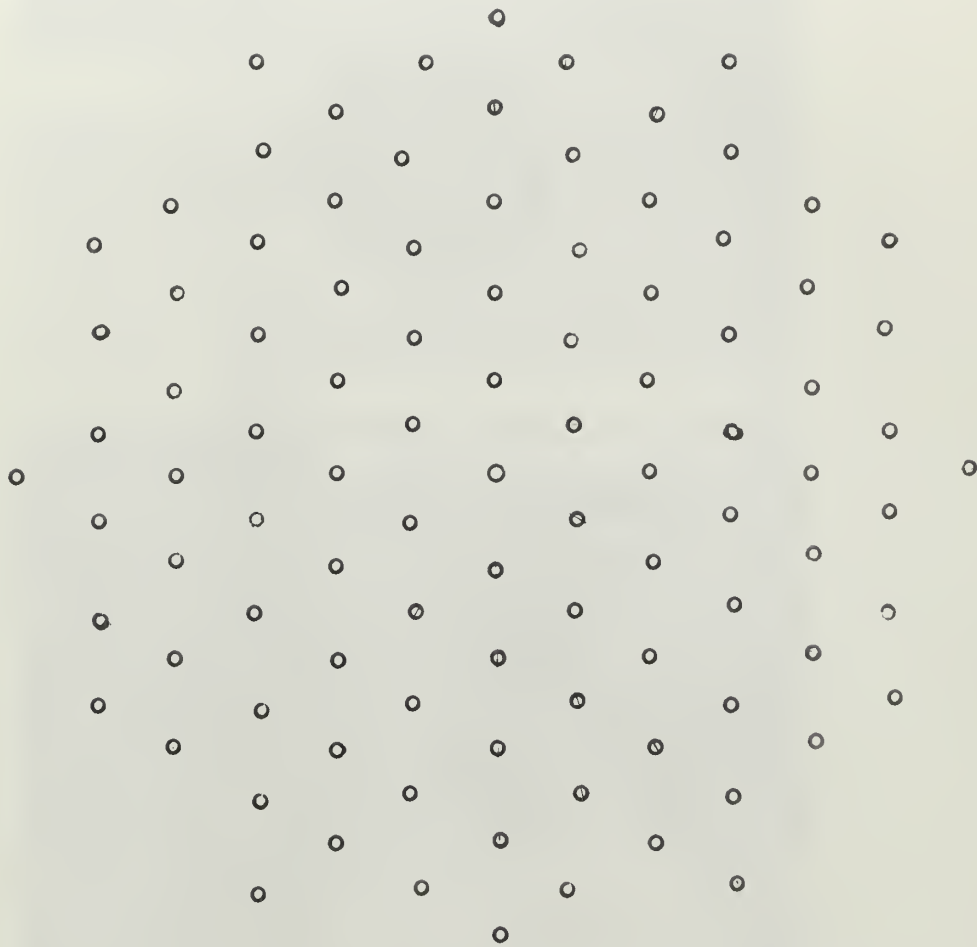


FIGURE 5. THERMOCOUPLE CONTROL SYSTEM



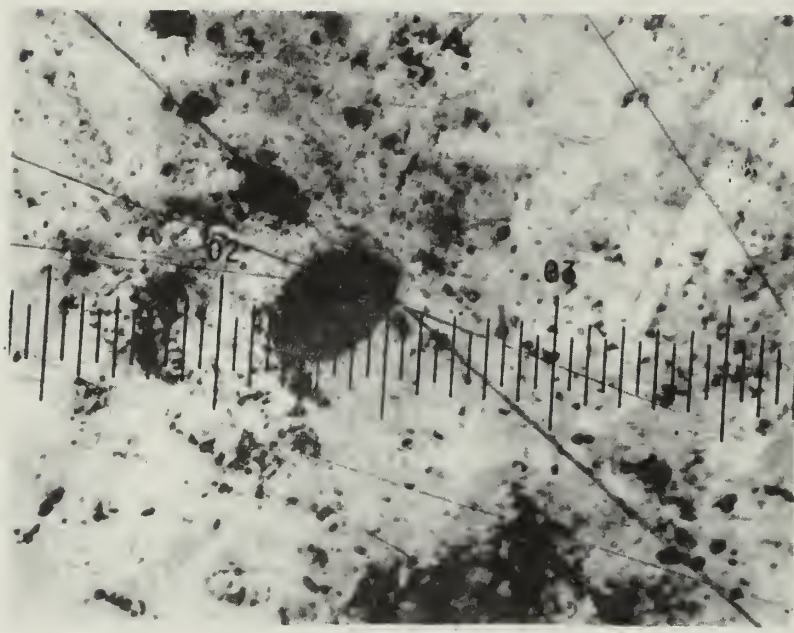
HOLE DIAMETERS=0.015

FIGURE 6. LAYOUT OF THIRTEEN DRILLED CAVITIES



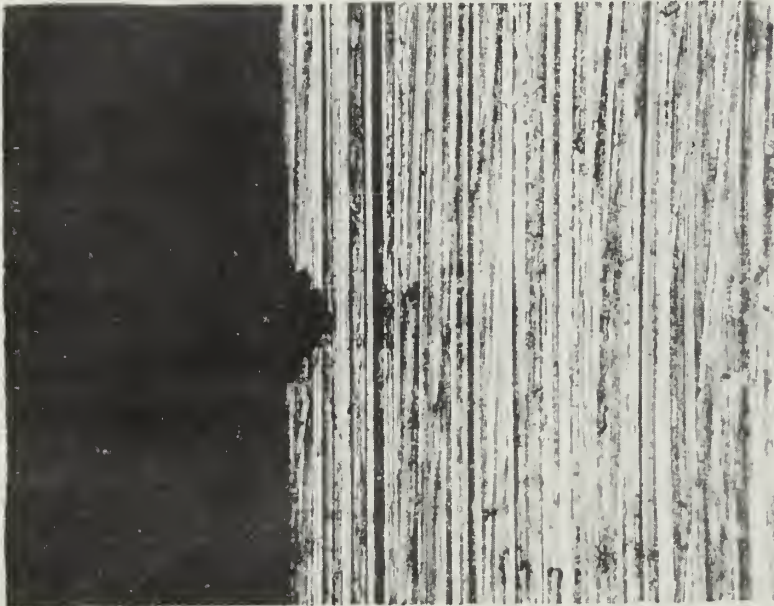
HOLE SPACING=0.095

FIGURE 7. LAYOUT OF 97 SPARK CUT CAVITIES



MAGNIFICATION=100X

FIGURE 11. MICROGRAPH OF A METAL PARTICLE



1971-1972

1. 1971-1972

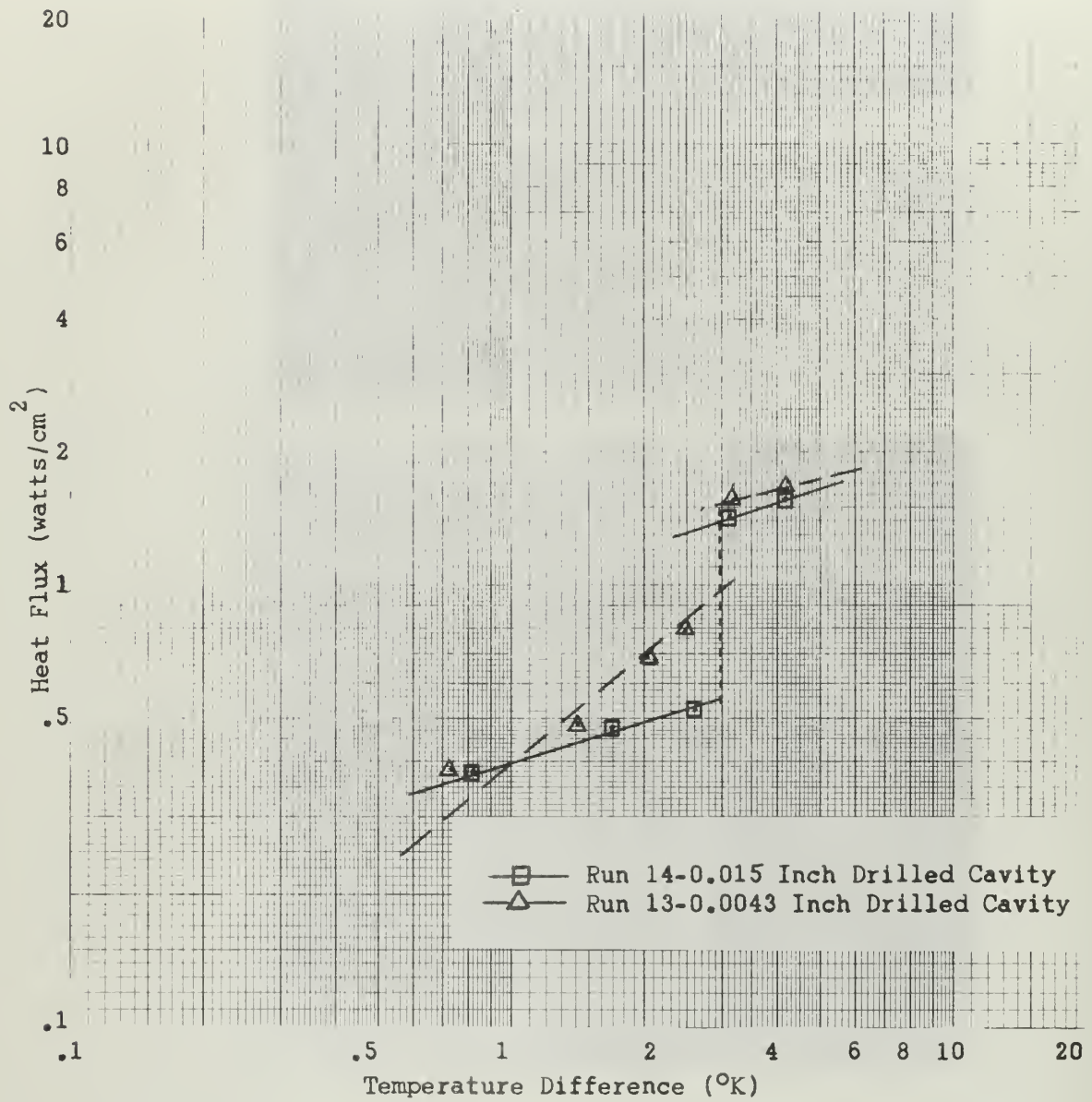


FIGURE 10. NATURAL CONVECTION DATA SHOWING JUMP EFFECT OBTAINED WITH SINGLE DRILLED CAVITIES



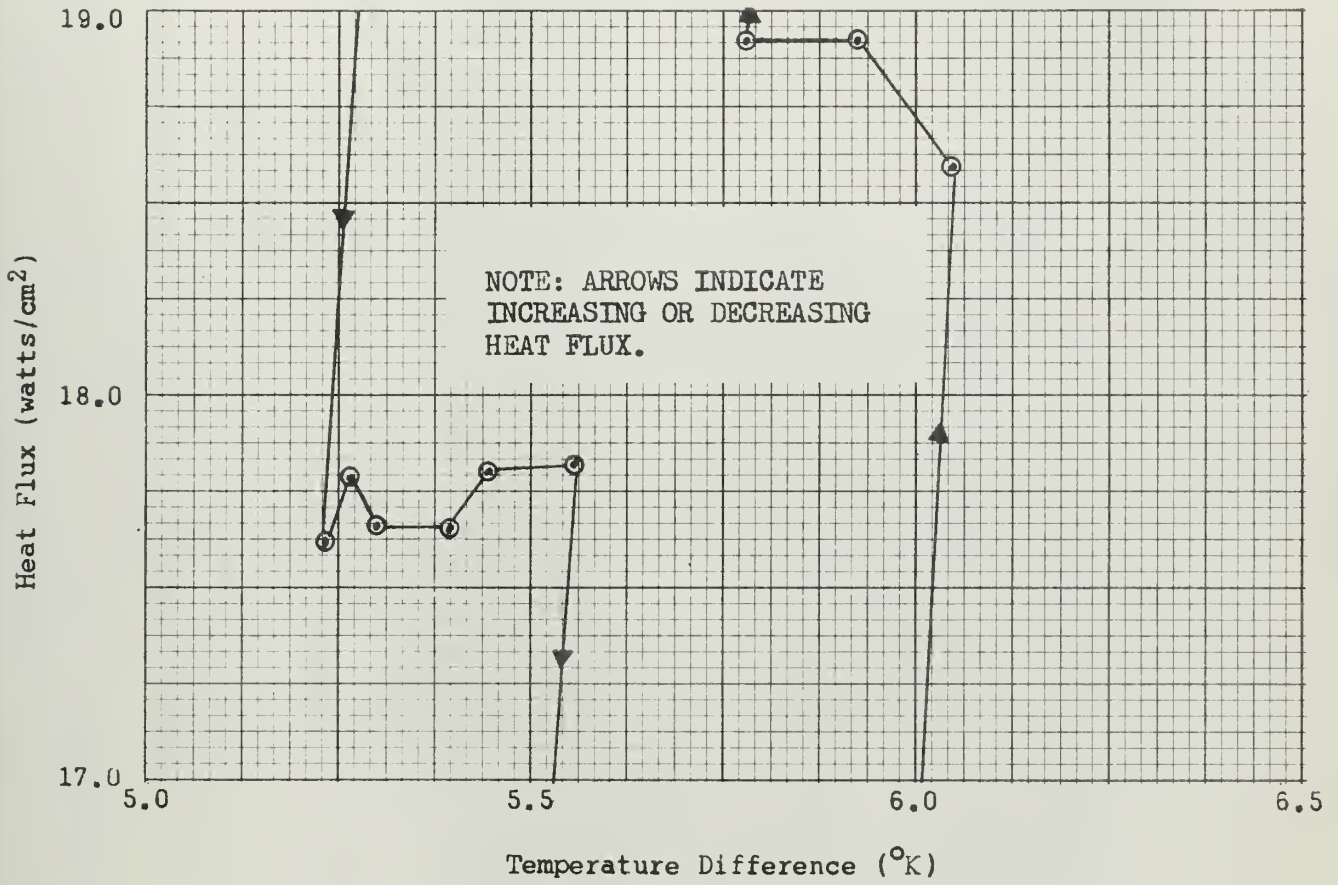


FIGURE 11. TIME-TEMPERATURE-HEAT FLUX PLOT

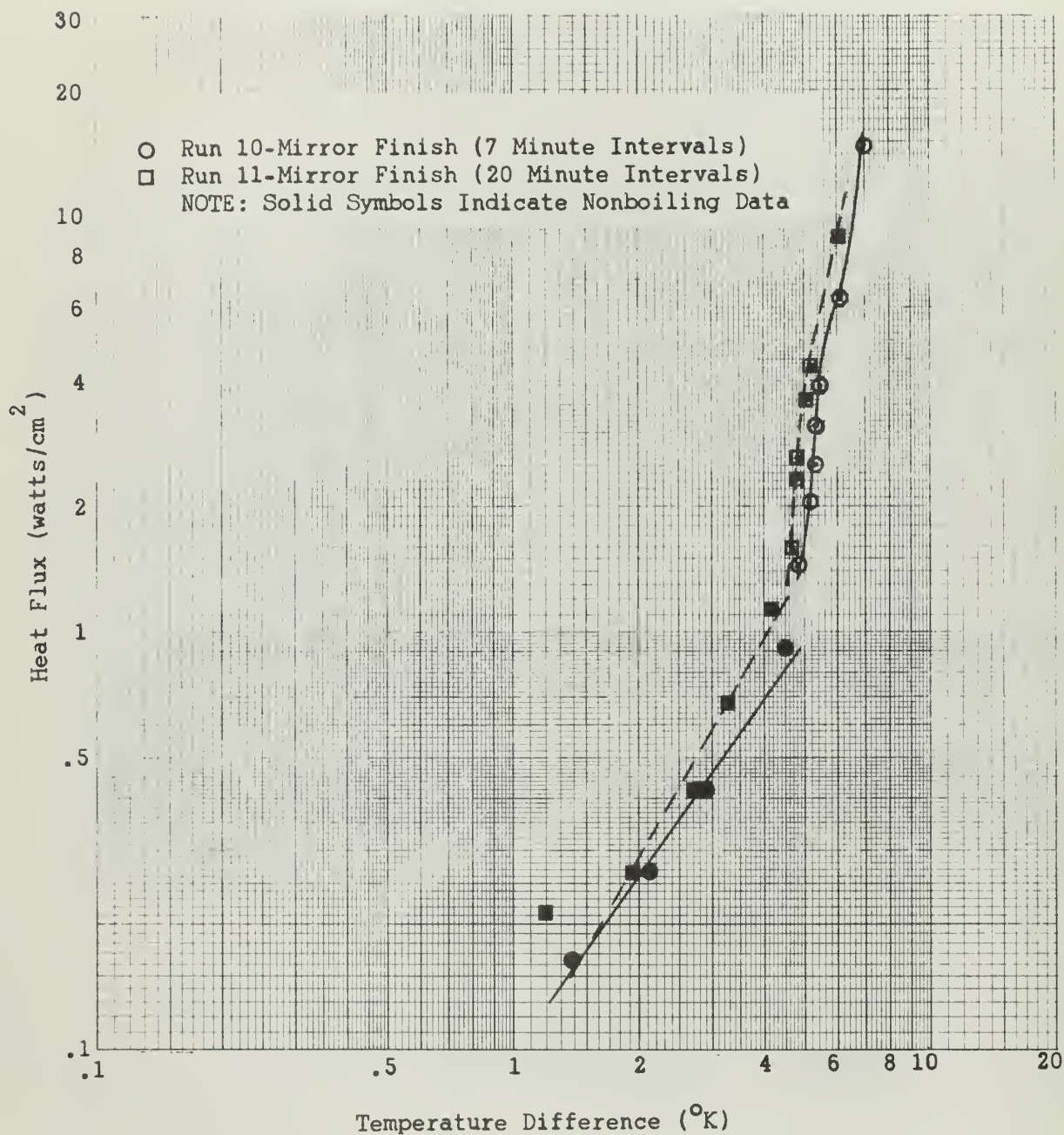


FIGURE 12. EFFECT ON THE BOILING CURVES OF DIFFERENT TIME INTERVALS BETWEEN POWER LEVEL CHANGES

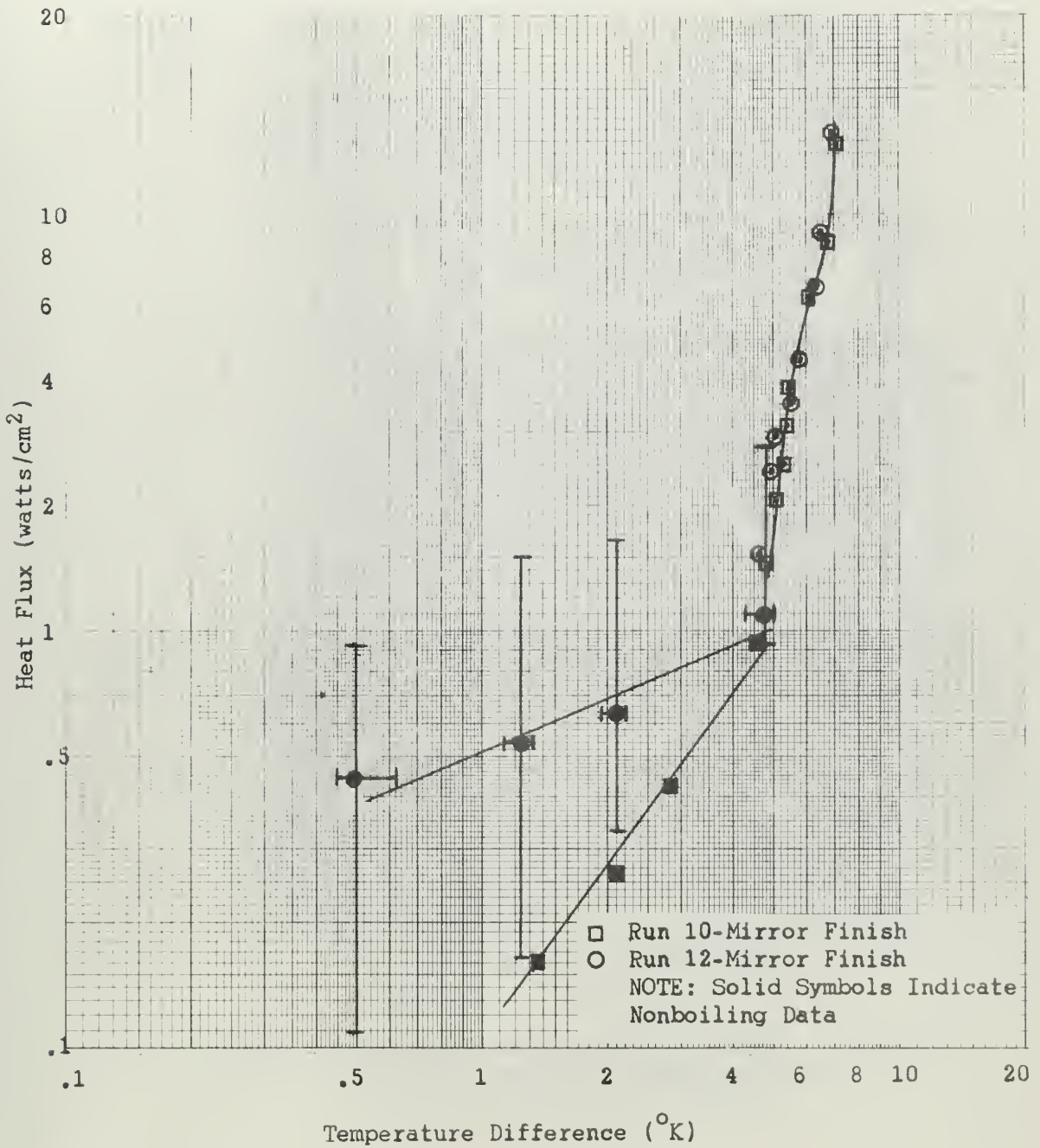


FIGURE 13. CURVE SHOWING REPRODUCIBILITY OF BOILING DATA USING MIRROR FINISH SURFACES

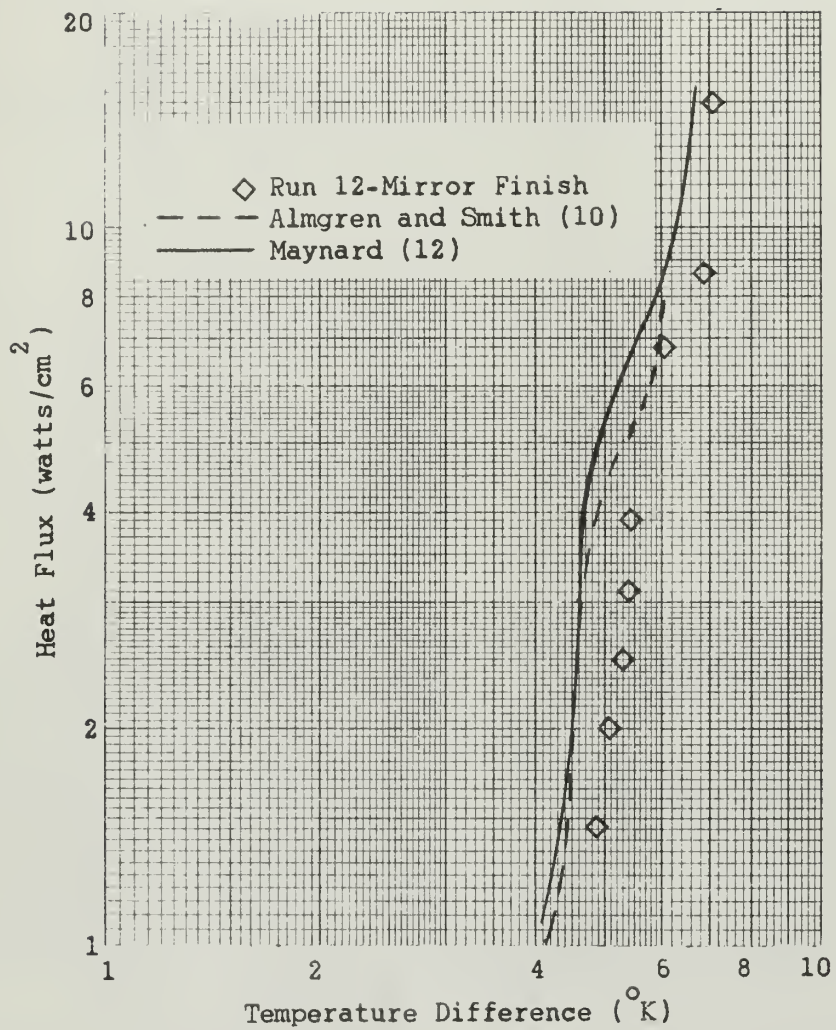


FIGURE 14. MIRROR FINISH BOILING CURVE SHOWING OTHER EXPERIMENTERS' MIRROR FINISH DATA

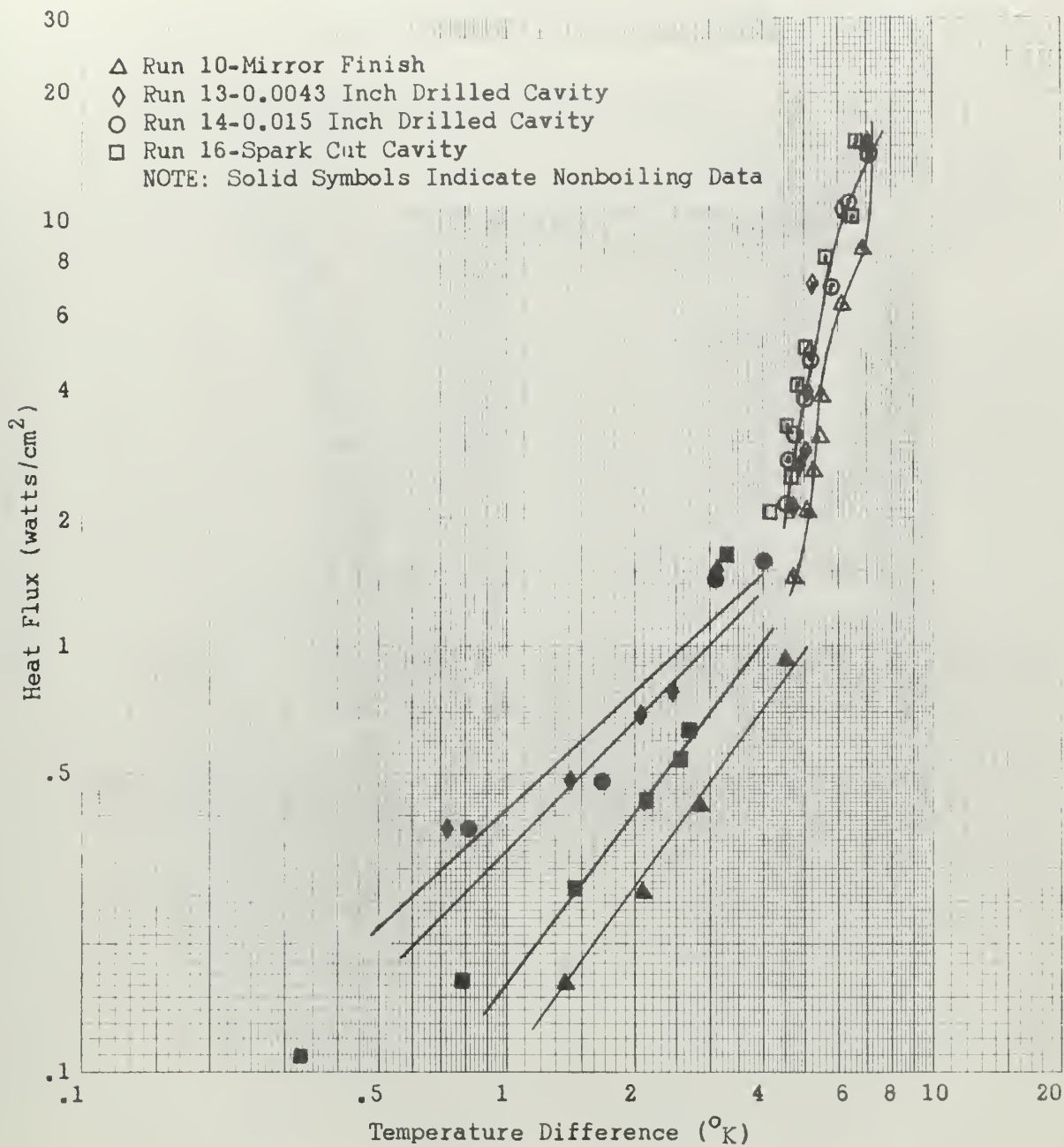


FIGURE 15. EFFECT ON THE BOILING CURVE OF DIFFERENT SIZES OF CYLINDRICAL CAVITIES

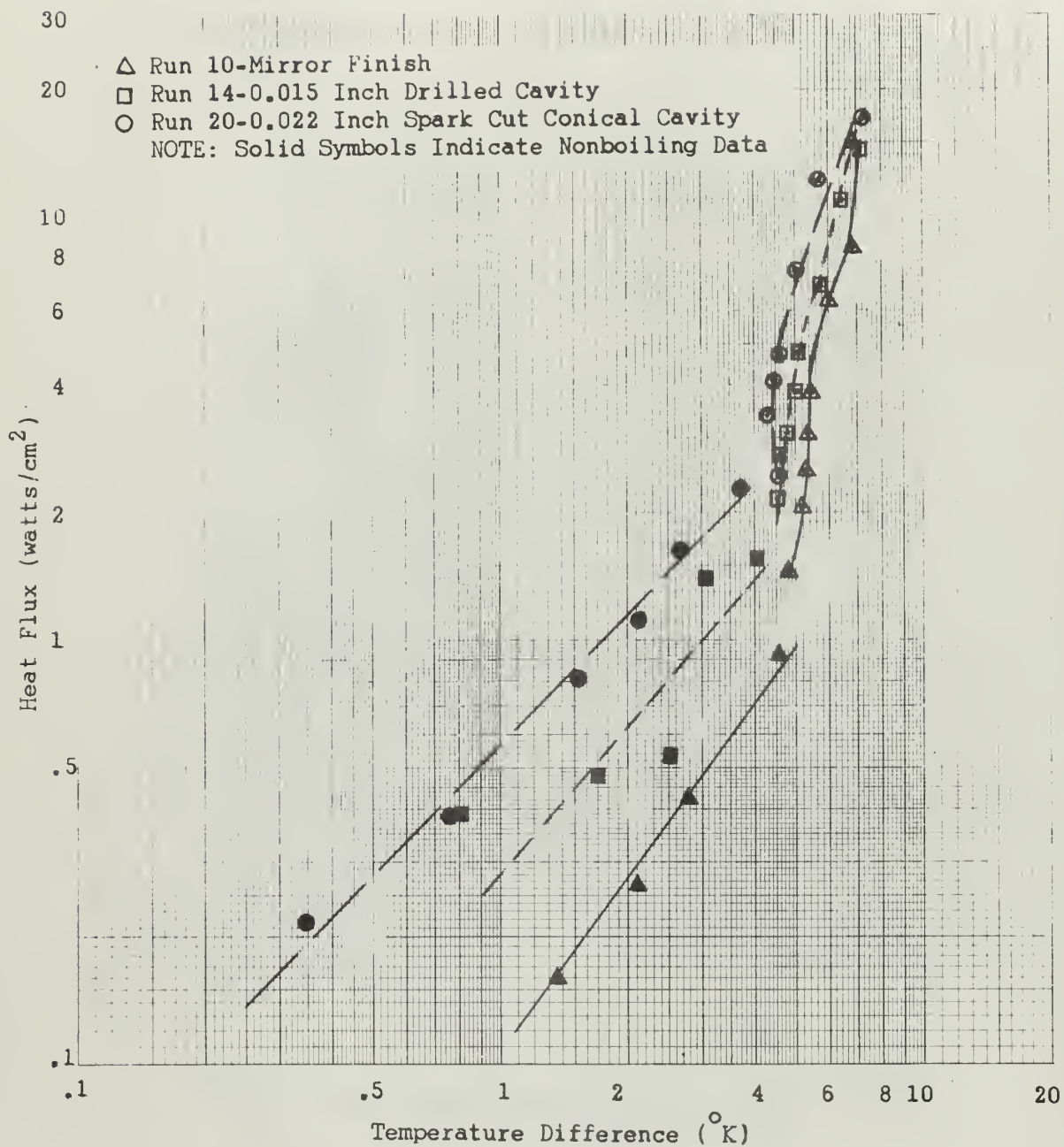


FIGURE 16. EFFECT OF CAVITY GEOMETRY ON THE BOILING CURVE

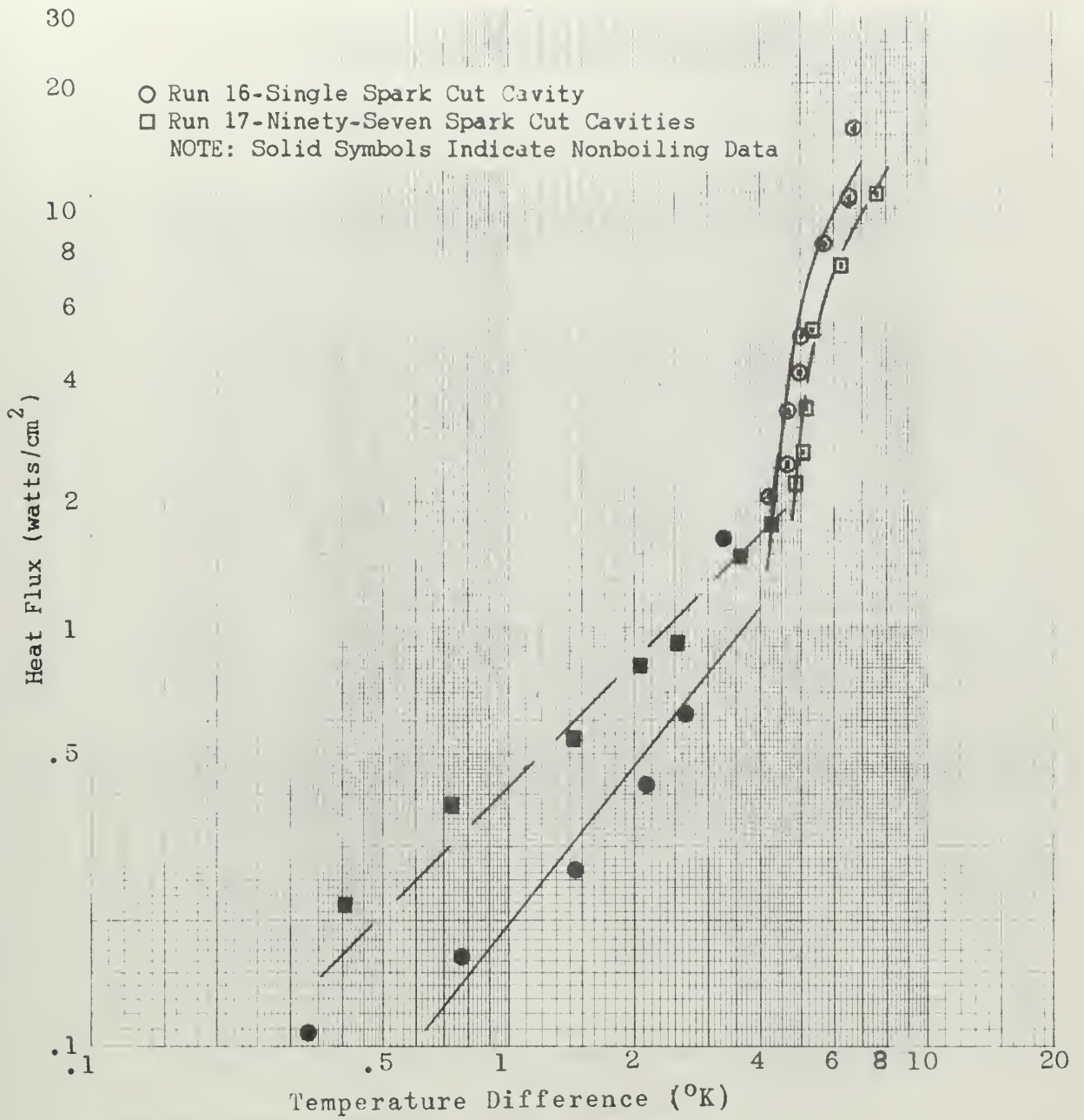


FIGURE 17. EFFECT OF SPARK CUT CAVITIES ON THE BOILING CURVE

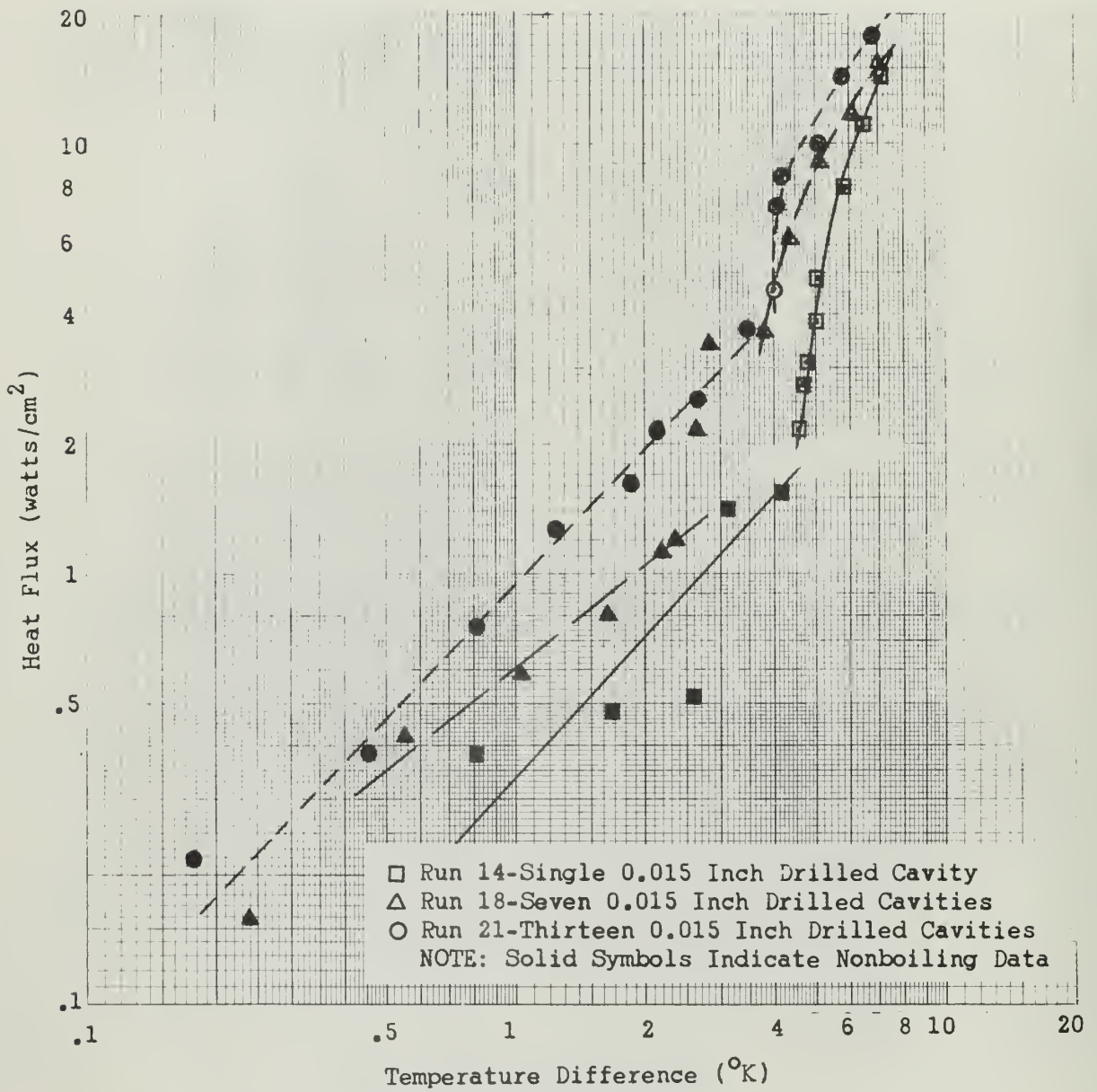


FIGURE 18. EFFECT OF NUMBER OF DRILLED CAVITIES ON THE BOILING CURVE



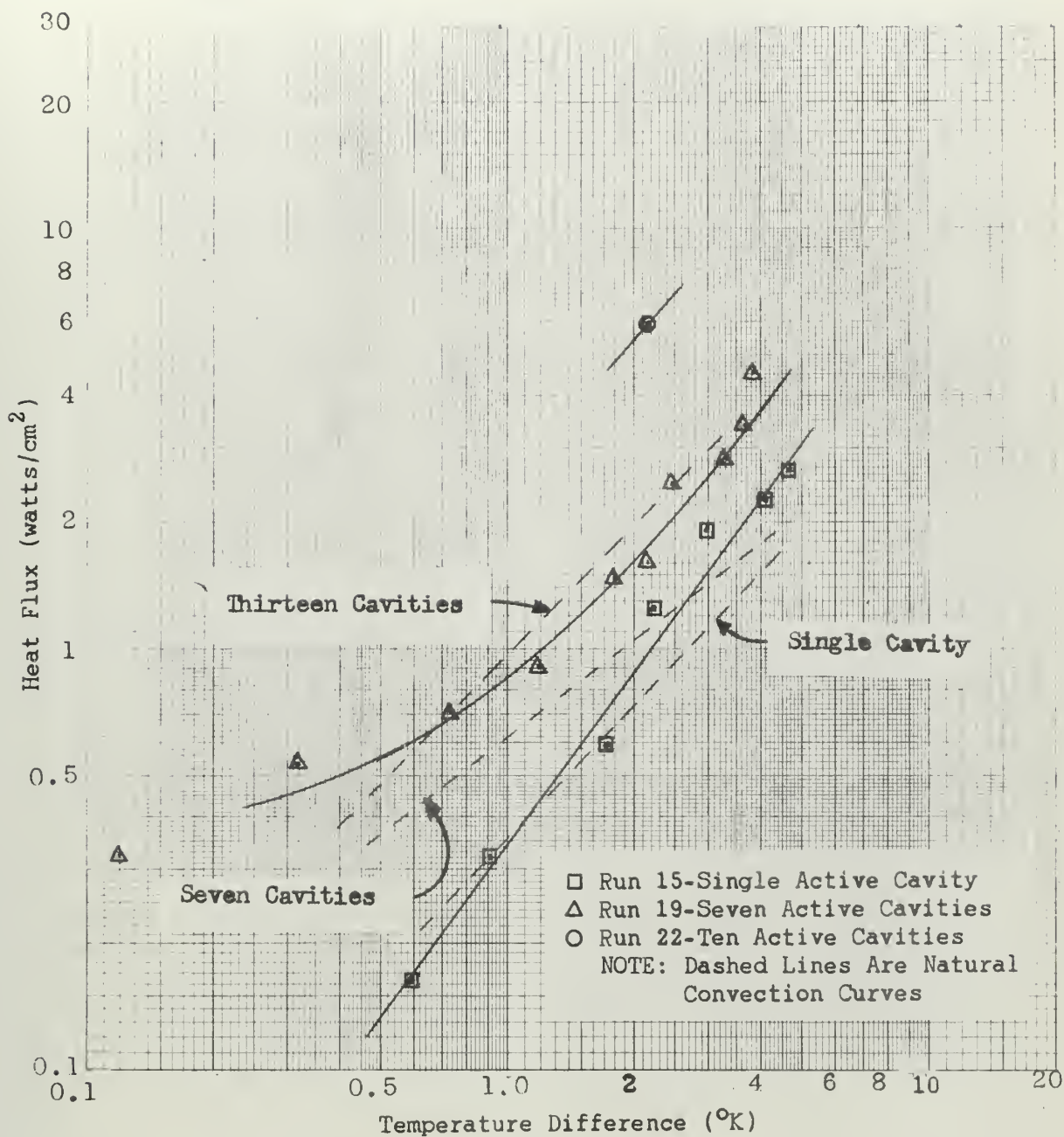


FIGURE 19. COMPARISON OF BOILING ONLY FROM ARTIFICIAL CAVITIES TO NATURAL CONVECTION CURVES

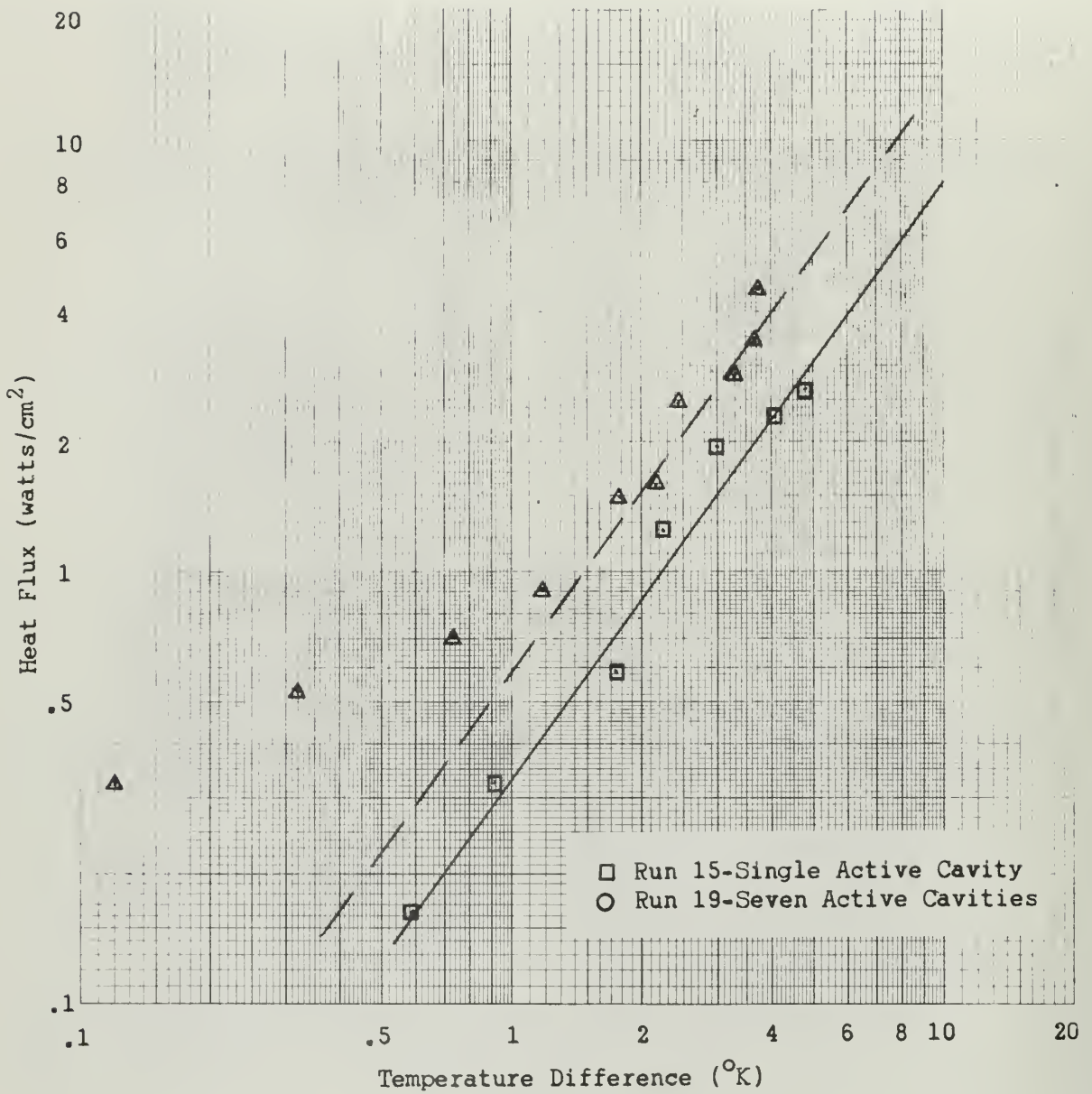


FIGURE 20. BOILING ONLY FROM ARTIFICIAL CAVITIES DATA SHOWING CURVES OBTAINED USING YAMAGATA'S EQUATION

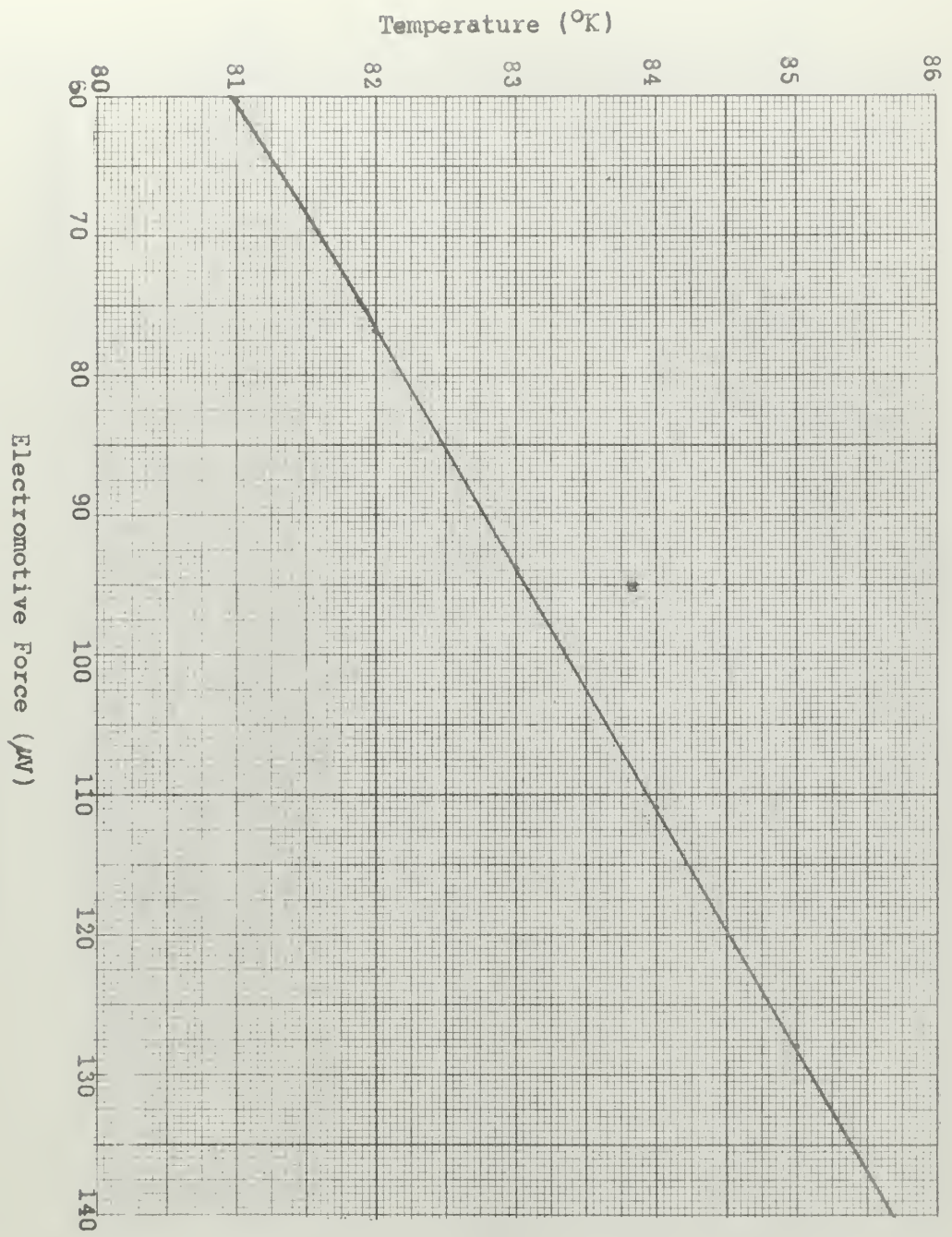


FIGURE 21. SAMPLE TEMPERATURE-EMF CURVE

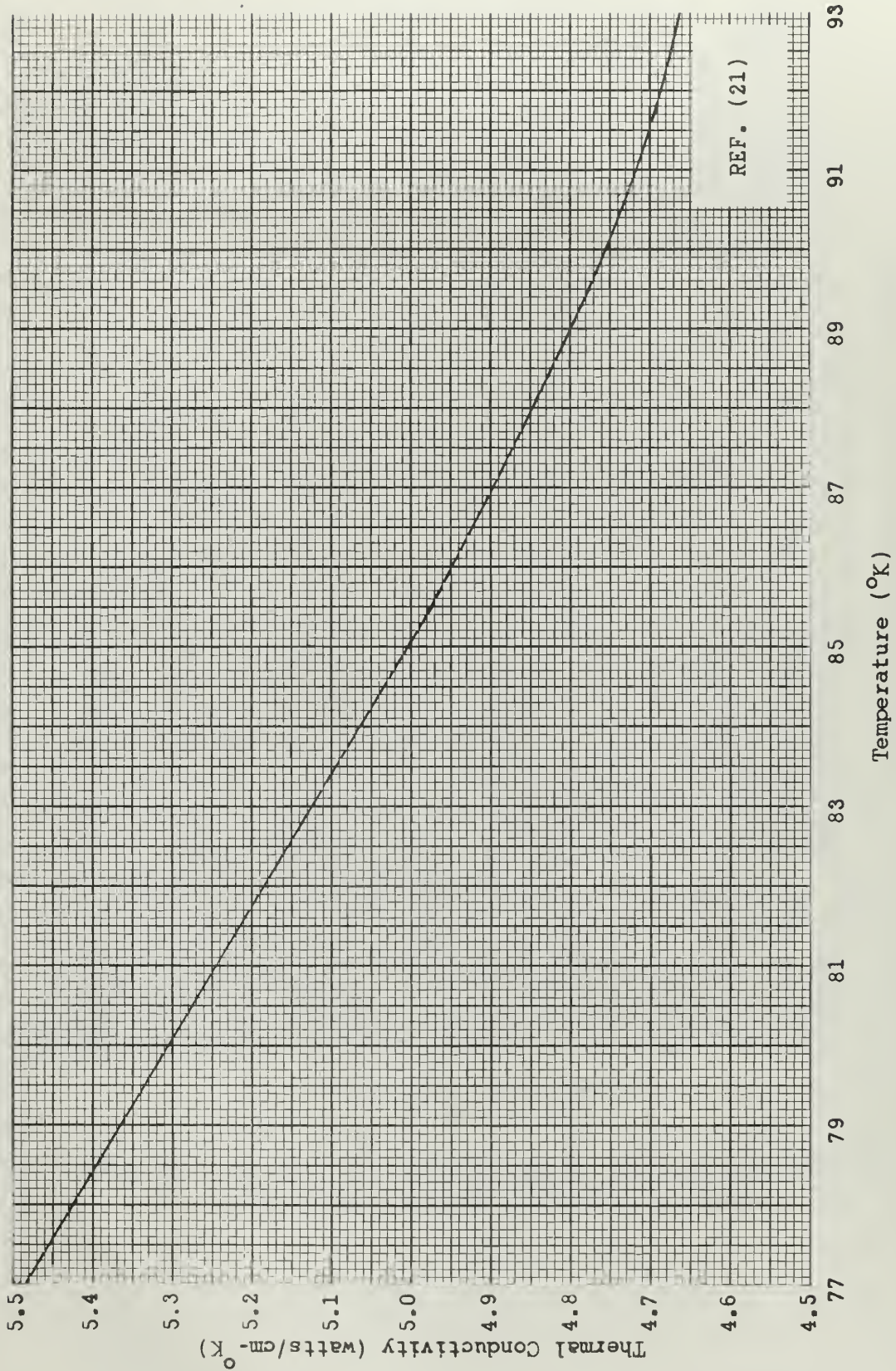


FIGURE 22. THERMAL CONDUCTIVITY OF COPPER

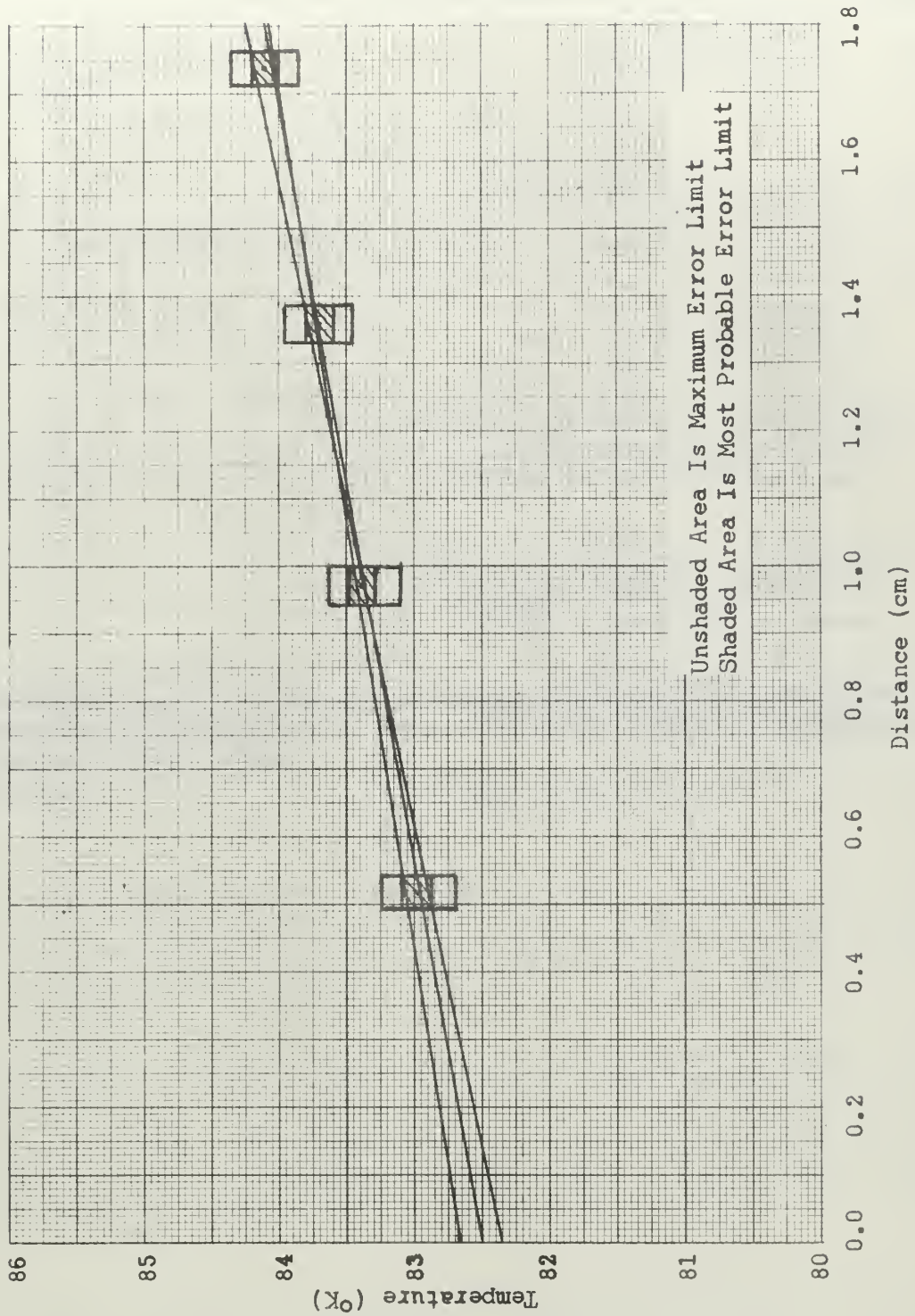


FIGURE 23. TEMPERATURE DISTRIBUTION IN THE BOILER CYLINDER

INITIAL DISTRIBUTION LIST

	<u>No. Copies</u>
1. Defense Documentation Center Cameron Station Alexandria, Virginia 22314	20
2. Library Naval Postgraduate School Monterey, California 93940	2
3. Mechanical Engineering Department Naval Postgraduate School Monterey, California 93940	1
4. Professor P. J. Marto Mechanical Engineering Department Naval Postgraduate School Monterey, California 93940	5
5. LT J. A. Moulson, USN Pearl Harbor Naval Shipyard FPO San Francisco	1

## Security Classification

## DOCUMENT CONTROL DATA - R&amp;D

(Security classification of title, body of abstract and indexing annotation must be entered when the overall report is classified)

1. ORIGINATING ACTIVITY (Corporate author) NAVAL POSTGRADUATE SCHOOL MONTEREY, CALIFORNIA 93940		2a. REPORT SECURITY CLASSIFICATION UNCLASSIFIED	
		2b. GROUP	
3. REPORT TITLE NUCLEATE POOL BOILING OF NITROGEN FROM ARTIFICIAL CAVITIES			
4. DESCRIPTIVE NOTES (Type of report and inclusive dates) THESIS			
5. AUTHOR(S) (Last name, first name, initial) MOULSON, JOHN A., LT, USN			
6. REPORT DATE SEPTEMBER 1967		7a. TOTAL NO. OF PAGES 83	7b. NO. OF REFS 26
8a. CONTRACT OR GRANT NO.		9a. ORIGINATOR'S REPORT NUMBER(S)	
b. PROJECT NO.			
c.		9b. OTHER REPORT NO(S) (Any other numbers that may be assigned this report)	
d.			
10. AVAILABILITY/LIMITATION NOTICES <del>THIS DOCUMENT IS UNCLASSIFIED</del> <del>EXCEPT WHERE SHOWN OTHERWISE</del> <del>IT IS TO BE DISTRIBUTED UNLIMITEDLY</del>			
11. SUPPLEMENTARY NOTES		12. SPONSORING MILITARY ACTIVITY	
13. ABSTRACT Pool boiling heat transfer of nitrogen from artificial cavities was investigated. Boiling was from circular, one inch diameter horizontal mirror finished copper plates.  The single artificial cavity surfaces investigated were: a drilled 0.0043 inch diameter hole, a drilled 0.015 inch diameter hole, an 0.022 inch diameter spark cut cone, and an 0.006 inch diameter spark cut cylindrical hole. The multiple cavity surfaces investigated were: seven 0.015 inch diameter drilled holes, thirteen 0.015 inch diameter drilled holes, and ninety-seven 0.003 to 0.0045 inch diameter spark cut holes. The depth to diameter ratio was about 2.5 for all drilled cavities.  The data from a mirror finished surface was compared to that of previous investigations. Exponents for Yamagata's Equation for boiling in the isolated bubble region were determined. The artificial cavities were found to affect the natural convection heat transfer. The size of the cavity appeared to have little effect after incipience of boiling, and larger cavities than previously expected were found to remain active.			

14

KEY WORDS

LINK A

LINK B

LINK C

ROLE

WT

ROLE

WT

ROLE

WT

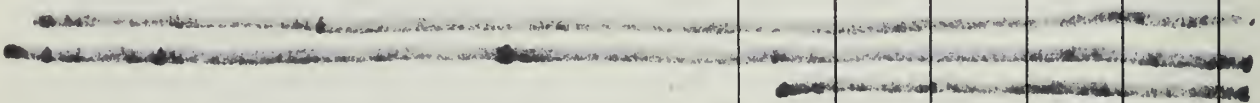
Nucleate boiling

Natural convection

Liquid Nitrogen

Cavities

Hysteresis















thesM855

Nucleate pool binding of nitrogen from

DUDLEY KNOX LIBRARY



3 2768 00421947 7

DUDLEY KNOX LIBRARY